Journal of Magnetism and Magnetic Materials 320 (2008) 2547–2562

Contents lists available at ScienceDirect

Journal of Magnetism and Magnetic Materials

journal homepage: www.elsevier.com/locate/jmmm

Topical Review

Superconducting vortex pinning with artificial magnetic nanostructures

M. Vélez [a,*], J.I. Martín [a], J.E. Villegas [b,c], A. Hoffmann [d], E.M. González [e], J.L. Vicent [e], Ivan K. Schuller [f]

[a] Depto. Física, Universidad de Oviedo-CINN, Av. Calvo Sotelo s/n, 33007 Oviedo, Spain
[b] Unité Mixte de Physique CNRS/Thales, RD 128, 91767 Palaiseau, France
[c] Université Paris Sud 11, 91405 Orsay, France
[d] Materials Science Division, Center for Nanoscale Materials, Argonne National Laboratory, Argonne, IL 60439, USA
[e] Depto. Física de Materiales, F. Fisicas, Universidad Complutense de Madrid, 28040 Madrid, Spain
[f] Physics Department, University of California, 9500 Gilman Drive, La Jolla, San Diego, CA 92093-0319, USA

ARTICLE INFO

Article history:
Received 26 February 2008
Received in revised form
6 June 2008
Available online 18 June 2008

PACS:
75.75.+a
74.78.Db
74.25.Qt

Keywords:
Superconducting thin film
Magnetic nanostructure
Vortex pinning

ABSTRACT

This review is dedicated to summarizing the recent research on vortex dynamics and pinning effects in superconducting films with artificial magnetic structures. The fabrication of hybrid superconducting/magnetic systems is presented together with the wide variety of properties that arise from the interaction between the superconducting vortex lattice and the artificial magnetic nanostructures. Specifically, we review the role that the most important parameters in the vortex dynamics of films with regular array of dots play. In particular, we discuss the phenomena that appear when the symmetry of a regular dot array is distorted from regularity towards complete disorder including rectangular, asymmetric, and aperiodic arrays. The interesting phenomena that appear include vortex-lattice reconfigurations, anisotropic dynamics, channeling, and guided motion as well as ratchet effects. The different regimes are summarized in a phase diagram indicating the transitions that take place as the characteristic distances of the array are modified respect to the superconducting coherence length. Future directions are sketched out indicating the vast open area of research in this field.

1. Introduction

Vortex pinning in type-II superconductors has been studied for a long time, both in conventional [1] and high-temperature superconductors (HTSC) [2], to develop a fundamental understanding of flux dynamics and, for its relevance in applications requiring enhancements of the critical current densities. Thus, several types of artificial pinning centers have been introduced in a controlled way in the superconductors; they usually consist of imperfections in the superconductor arranged either randomly or in ordered configurations. Among the randomly distributed defects [3–5], cold work-induced dislocations [6], secondary-phase precipitates [7], or heavy-ion radiation-induced defects [8] exhibit suitable properties as pinning centers. Pinning effects by ordered arrays of defects have been intensively studied for several decades; first, with defects of lateral size in the micron range, like arrays of holes [9], holes in superconducting networks [10], or magnetic particles [11,12]. More recently, the development of new lithography techniques has allowed the reduction of the size, using submicron defects such as arrays of holes [13] or spatially modulated e-beam irradiation damage with electron [14] or ion beams [15].

Vortex pinning by arrays of regular dots has relevance and may serve as ideal model systems to other fields of physics including vortex arrays in confined charged plasmas, epitaxial growth of elastically soft materials deposited on top of a rigid lattice, a variety of hybrid systems in which the proximity effect plays an important role, etc. Moreover, the relevant physics length scales are close to what can be artificially produced in the laboratory so this allows studies in which matching effects between structural and physics length scales occur. Since the array geometries can be manipulated at will and with the wealth of existing superconductors this provides a very rich system in which varying many of the relevant parameters allows to study the effect of thermal fluctuations, commensuration issues, interactions between different types of vortices (for instance magnetic and superconducting), etc. In addition, these systems provide the means for the development of novel devices such as tunable "Josephson like" systems [16–18], can be used as a tool to modify the field-dependent critical current of Josephson junctions [19–21], allow the reduction of noise in SQUID-based devices [22,23] and in microstrip band-pass filters [24], and open up the avenue for the enhancement of critical currents and current carrying capacity of superconducting cables and wires.

* Corresponding author. Tel.: +34 985102947; fax: +34 985102952.
E-mail address: mvelez@uniovi.es (M. Vélez).

0304-8853/$ - see front matter © 2008 Elsevier B.V. All rights reserved.
doi:10.1016/j.jmmm.2008.06.013

A case of particular interest is the one based on superconducting films with ordered arrays of magnetic dots with diameter of several hundreds of nanometers [25]. These sizes are comparable to typical characteristic lengths of conventional superconductors, such as the coherence length or the London penetration depth [26]. Moreover, the magnetic character of the dots can induce stronger pinning effects than similar nonmagnetic pinning centers [27] by locally degrading superconductivity around the magnetic dot through the magnetic proximity effects and stray fields (for a review on superconducting-ferromagnet systems, see e.g. Ref. [28]). In addition, large enough dot magnetization may create vortices in the superconducting film [29]. This has resulted not only in the observation of clear pinning effects when the vortex lattice interacts with high symmetry arrays of magnetic dots (triangular arrays [25,30], square [30,31] or kagomé [30] arrays), but also produced a rich behavior of the vortex dynamics that can be tuned by modifying the properties of the pinning array. It should be pointed out that, in order to understand vortex pinning with artificial arrays, it is necessary to consider the role played by individual dot properties such as size and/or magnetic state. In particular, the ability to tune *in situ* the pinning potentials via changes of the magnetic configuration presents a unique opportunity provided by magnetic pinning centers.

The reduction of dot-array symmetry from six-fold (triangular) or four-fold (square) to two-fold (rectangular [32]) results in a number of novel phenomena for the vortex-lattice movement in an anisotropic pinning potential. Further reduction of array geometry from periodic to quasiperiodic arrays of magnetic dots has also been realized with studies in two-dimensional (2D) Fibonacci arrays [33], pentagonal fractal arrays [33] and five-fold Penrose arrays of magnetized dots [34] yielding interesting changes on vortex pinning properties related to the range of correlations within the vortex lattice.

In addition, changes from circular to triangular shape of individual dots may induce interesting ratchet effects, in which a positive or negative rectification is obtained, depending on the magnitude of the AC drive and/or the strength of the applied magnetic field [35,36]. The vortex rectification can be further modified by changing the magnetic state of triangular rings [37,38].

This article is dedicated to review periodic pinning effects and the changes that appear in vortex dynamics in superconducting films with artificial magnetic structures composed mainly of submicrometric arrays of magnetic dots. Special emphasis is given to the role played by array symmetry and the relevant lengths and sizes.

This review is organized as follows; first, the fabrication of the magnetic nanostructures/superconducting films hybrids is described. Second, vortex dynamics in films with regular (triangular or square) arrays of magnetic dots are reviewed, indicating the role of relevant parameters such as the order in the array, magnetic character and sizes of the dots. Then, the new phenomena found as the symmetry of the magnetic dot arrays is distorted to become rectangular are discussed, including reconfigurations in the vortex lattice, anisotropic vortex dynamics, channelling and guided motion due to size effects. A phase diagram for vortex pinning regimes is presented that summarizes the transitions from one regime to another as the different distances of the array are changed relative to the superconducting coherence length. The consequences on the vortex dynamics produced by further reduction in the array symmetry including asymmetric and aperiodic pinning arrays are discussed. Finally, the future outlook and a number of interesting novel directions are outlined.

2. Fabrication of hybrid superconducting/magnetic nanostructures

The fabrication of hybrid superconducting/magnetic nanostructures for the study of periodic pinning effects usually relies on nanolithography techniques [39] to define submicrometric periodic arrays of pinning centers (i.e. of a size comparable with the characteristic lengths λ and ξ of the superconductor). One of the most widely used techniques has been e-beam lithography, because it allows control of array parameters (symmetry, lattice parameter, and particle size) at the micron and submicron length scales. In some cases, the magnetic nanostructure is prepared first on top of a Si substrate and, then, a superconducting film (usually Nb or Pb with a thickness in the range 10–100 nm) is deposited on top [40–42], whereas in other cases the reverse situation is preferred and the magnetic nanostructure is fabricated on top of a flat superconducting film [43]. Also, Bitter decoration technique and e-beam lithography have been used to create triangular and square arrays of magnetic particles on top of superconducting crystals ($NbSe_2$ or $Bi_2Sr_2CaCu_2O_8$) [44–46]. Metallic replica masks have been used to fabricate arrays of submicron Ni dots in high-temperature superconducting films [47] in order to avoid possible degradation during the e-beam lithography process.

Different materials have been used for the fabrication of the magnetic nanostructures such as SmCo [11,48], Ni [25,49], Fe [50], or Co [51] and, also perpendicular anisotropy Co/Pd and Co/Pt multilayers [43,52].

Different array geometries have been used in the study of periodic pinning, mainly composed of magnetic particles of size d arranged in different symmetry arrays: (a) regular such as periodic triangular, kagomé, or square, (b) distorted such as periodic rectangular lattices, and even (c) aperiodic arrays such as Fibonacci or Penrose lattices. In general, the most important geometrical parameter is the lattice parameter (a for triangular and square lattices or $a \times b$ for rectangular ones, see sketch in Fig. 1) and the area of the unit cell of the array, S_0.

The superconducting properties of the hybrid structures have been characterized either by; transport measurements (magnetoresistance, critical current and current voltage characteristics) [25,53], DC magnetization [30,51], AC susceptibility [54], or imaging techniques such as scanning Hall probe microscopy [42] and Lorentz microscopy [15].

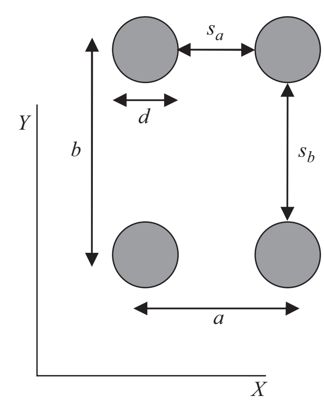

Fig. 1. Schematic of the rectangular array geometry indicating the definitions of the lattice parameters a and b along the X and Y axes. Also indicated is the dot diameter d and the different interdot separations s_a and s_b along a and b, respectively. Note that a square array of dots is just a particular case of the rectangular lattice with $a = b$.

3. Regular arrays of magnetic dots

3.1. Periodic pinning by regular arrays of weak pinning centers

In a uniform superconducting material, the minimum energy for a vortex lattice created by a magnetic field B corresponds to a triangular lattice of parameter

$$a_0 = 1.075(\Phi_0/B)^{1/2}$$

where $\Phi_0 = 2.07 \times 10^{-7}\,\mathrm{G\,cm^2}$ is the quantum of flux [26]. However, in the presence of a periodic array of defects, the vortex lattice can adopt different highly ordered configurations to take advantage of the periodic pinning potential when the number of vortices per unit cell of the array $n_\mathrm{v} = BS_0/\Phi_0$ is an integer or a fractional number [15,55,56]. This results in an enhanced pinning between the vortex lattice and the array of defects when a matching condition is fulfilled, giving rise to pronounced minima in the dissipation that have been observed in different symmetry regular arrays of magnetic dots, such as triangular [25,30], kagome [30], or square [30,31]. Fig. 2 shows the magnetoresistance $\rho(B)$ at $0.99T_\mathrm{C}$ of a 100 nm thick Nb film grown on top of a square array of Ni dots of lattice parameter $a = 400$ nm and dot diameter $d = 250$ nm, measured with different values of the applied transport current [53]. For a certain current range, clear magnetoresistance minima appear at equidistant magnetic field intervals, given by $B_\mathrm{n} = n\ B_1$, where $B_1 = 130$ G is the so-called "first matching field". This closely corresponds to a single vortex per unit cell $n_\mathrm{v} = B_1 a^2/\Phi_0 = 130\,\mathrm{G} \times (400\,\mathrm{nm})^2/\Phi_0 = 1.005$.

Periodic pinning anomalies are also observed either as peaks or plateaus in the critical current vs. field curves [30] and in the magnetization curves close to $T_{\mathrm{C}51}$ both at integer and fractional multiples of the matching field. At lower temperatures, this periodic structure disappears. However, below approximately 4 K, the presence of the periodic arrays of magnetic dots becomes noticeable again as quasiperiodic instabilities (flux jumps) in the isothermal magnetization curves of the superconducting thin films [48,57]. Taking into account the gradient in vortex density across the sample due to the critical state, these results suggest that the matching between the vortex lattice and the periodic array occurs essentially in "terraces" of matched vortex density near the film edge.

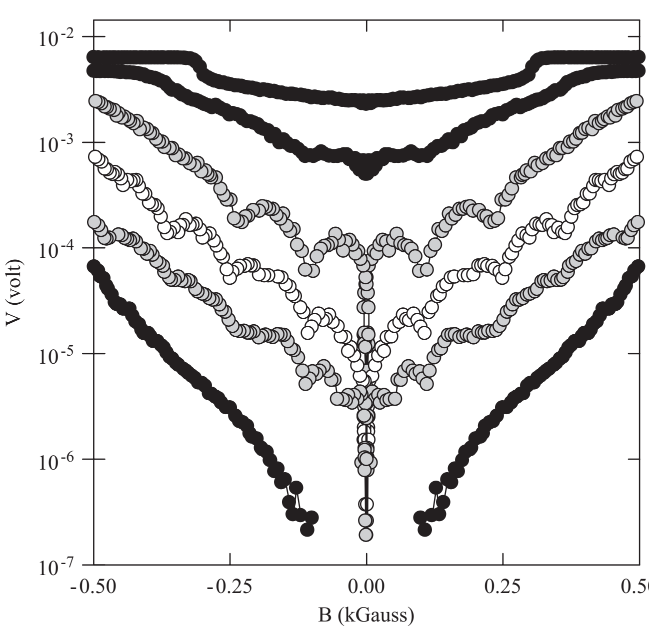

Fig. 2. Voltage vs. field for a 100 nm thick Nb film with a square (400 nm × 400 nm) array of Ni dots at $0.99T_\mathrm{C}$: A, $J = 10^4\,\mathrm{A/cm^2}$; B, $J = 7.5 \times 10^3\,\mathrm{A/cm^2}$; C, $J = 5 \times 10^3\,\mathrm{A/cm^2}$; D, $J = 3.75 \times 10^3\,\mathrm{A/cm^2}$; E, $J = 2.5 \times 10^3\,\mathrm{A/cm^2}$; F, $J = 1.25 \times 10^3\,\mathrm{A/cm^2}$ (after Martin et al. [53]).

The structure of the pinned vortex lattice depends on the balance of pinning energy by the regular array of defects and intervortex repulsion that favors a triangular lattice. The rich vortex-lattice phase diagrams have been simulated using numerical methods in square lattices of pinning centers [58], in which many different vortex phases appear ranging from square-pinned for strong pinning centers to distorted-triangular for weak pinning centers [59].

It is interesting to note that controlled disorder in the dot positions within the square array of Ni dots [60], conserves the resistivity minimum at the first matching whereas the higher order periodic pinning become gradually washed out, indicating the relevance of interstitial pinning when there is more than one vortex per dot.

The thickness range over which the periodic pinning potential created by a square array of Fe dots fabricated on a $Bi_2Sr_2CaCu_2O_8$ single-crystal surface [50] can influence the structure of the vortex lattice has also been studied by Bitter decoration experiments on the top/bottom crystal surfaces. It was found that the square distortion induced by the ordered pinning array was only relevant for thicknesses below approximately 1 μm, which was close to the penetration depth at the measurement temperature.

3.2. Ordered artificial vs. random intrinsic pinning centers

In general, the ordered magnetic dot array that produces the periodic pinning potential competes with random defects present in the sample that tend to disorder the vortex lattice. Thus, for strong enough artificial pinning produced by the magnetic dot array, both resistivity minima and critical current maxima are observed [30,51]. In other cases, only resistivity minima might be observed in an optimal current range, as is the case for the data of Fig. 2 [25,53]. The current dependence of the matching effect is due to the order in the dynamical phases produced by the driving force magnitude and direction [61], which move the vortex lattice in the presence of the periodic pinning potential. Thus, enhanced matching in an optimal current range can be attributed to the onset of quasi long range order in the vortex lattice in a range of vortex velocities which promote the interaction with the periodic pinning potential [62]. Another signature of this competition between random and ordered pinning centers is that the periodic resistivity minima (critical current maxima) generally appear at temperatures close to the superconducting critical temperature [25,30,48,49,51] where random pinning becomes weaker and vortex mobility is higher.

An alternative way to study the interplay between ordered artificial and random intrinsic pinning centers [44] is using "double decoration". In these experiments, first an almost periodic triangular array of Fe particles is created on top of the superconductor using Bitter decoration of the vortex lattice. A second decoration is then used to observe the vortex lattice. These results show that periodic pinning is much more effective after dynamical order is induced in the vortex lattice [44,45]. Numerical simulations have also reproduced the experimentally observed crossover from individual pinning by each Fe particle in the strong pinning regime, to collective pinning only in the ordered regions for weaker pinning forces [63].

Finally, for samples in which random and ordered pinning potentials coexist, the vortex glass transition temperature is enhanced at the matching fields and the critical exponents are modified [64].

3.3. Magnetic character of the pinning interaction

Qualitatively similar matching effects have been observed in samples with arrays of nonmagnetic artificial pinning centers such as thickness modulations [65], radiation defects [15], antidots [13,66–69], blind holes [70], periodic corrugations [71], and nonmagnetic metallic dots [49,72]. However, a comparison of Ni with Ag dot [31,49] arrays of similar geometries shows a more effective pinning for the samples with magnetic (Ni) dots. Fig. 3 shows the highest order matching minima in the $\rho(B)$ curve, n_{max}, as a function of dot diameter for several Nb samples with ($400\,nm \times 400\,nm$) square arrays of Ni dots (solid symbols) or Ag dots (open symbols) [49]. In all the cases, the maximum number of matching minima is significantly larger in the samples with magnetic dots.

Different mechanisms can account for the pinning interaction between a ferromagnetic dot and a superconducting vortex [29,73] such as by the local superconductivity suppression due to the proximity effect (see Ref. [74]), and by the influence of the dot stray field [75]. For example, for in-plane magnetized Ni dots, the temperature dependence of the critical current can be explained by a combination of the proximity effect and the interaction between the vortex field and the magnetic moment of the dot [53]. Calculations in the London limit of vortex interactions either with dipoles [75–78], ferromagnetic columnar defects [79] and uniformly magnetized dots [80–82] via the vortex magnetic field have shown the relevance of the dot stray field as a source of tunable magnetic pinning. In particular, it has been shown [78] that the interaction energy between a superconducting vortex and a point dipole is given by — mb^{vac} where m is the magnetic moment and b^{vac} is the magnetic field created by the vortices at the dipole position.

This implies that the periodic pinning induced by magnetostatic interactions is strongly dependent on the dot magnetization. Since typical matching fields for array lattice parameters in the 1000–100 nm range are of the order of 100 Oe, smaller than the fields needed to significantly alter the dot magnetization, the pinning potential can be adjusted by preparing the remanent configuration of the dot array following different demagnetization processes above the superconductor critical temperature. For example, an enhanced periodic pinning has been observed for single domain as compared with multidomain dots for arrays of rectangular-shaped Co dots with in plane magnetization [51,83]. Scanning Hall probe microscopy experiments in these arrays [42] have shown that the vortices are attracted to a specific pole of the single domain rectangular dots depending on the applied field direction.

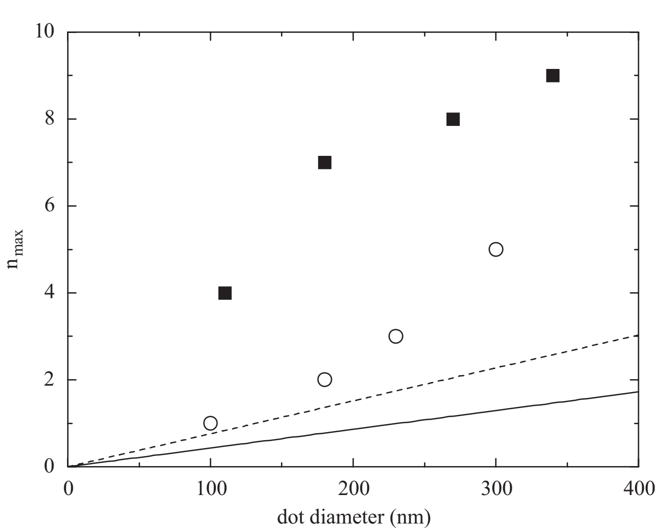

Fig. 3. Highest order n_{max} of observed matching peaks in the magnetoresistance curves as a function of dot diameter for 100 nm thick Nb films with ($400\,nm \times 400\,nm$) square arrays of: Ag dots (open symbols) or Ni dots (solid symbols). Lines indicate the saturation number for an insulating inclusion of diameter d for $\xi = 58\,nm$ (corresponding to $0.98T_C$, solid line) and $\xi = 33\,nm$ (corresponding to $0.94T_C$, dashed line) (after Hoffmann et al. [49]).

The pinning properties of arrays of Co and permalloy circular dots whose aspect ratio favors the formation of the so-called "magnetic vortex state" [84] have been recently investigated. The "magnetic vortices" in the nanodots induce several pinning mechanisms. First, the highly localized out-of-plane stray field of the "magnetic vortex" core results in a local suppression of superconductivity [85], which yields enhanced periodic pinning [86]. Second, using appropriate structures [225], dipolar magnetic interactions with "magnetic vortices" become the governing pinning mechanism. This allows to obtain a *switchable* pinning landscape, controllable via the magnetic history [87], and gives raise to asymmetric pinning, in a similar way as observed for systems with out-of-plane anisotropy [30].

Experiments have also been performed in superconducting films with arrays of triangular microloops, in which eight different remanent domain configurations can be selected (six of them polarized and two of them in the vortex state) [37,38]. In this way, both the strength of the pinning potential (weak for the low stray field flux-closure states and strong for the polarized states) and the symmetry of the pinning potential can be tuned *in situ*.

Out of plane magnetized dots produce asymmetric pinning, which depends on the relative alignment between the dot magnetic moment and the applied magnetic field that creates the vortices in the superconductor [30,52]. Stronger maxima are observed in the critical current for a parallel than for an antiparallel alignment. In agreement with this, scanning Hall probe microscopy shows that in the parallel case the vortices are strongly pinned at the dots, whereas in the antiparallel one they occupy weaker pinning interstitial positions [88]. Vortex dynamics simulations show that the pinning can be tuned from asymmetric to symmetric by changing the order of magnetic dipoles from ferromagnetic to antiferromagnetic [89,90]. Another interesting effect that appears for strong enough dot magnetization and/or large enough size is the nucleation of vortex–antivortex pairs in the superconducting film [80–82,91–95] giving rise to a variety of interesting phenomena. For small dot sizes, multiquanta vortices occur, whereas for larger dots (radius above 6ξ) ordered configurations of single quantum vortices may appear at each dot [82]. Also, the antivortices adopt interstitial positions and crystallize into different kinds of regular lattices [96–99]. Moreover, the stray field created by an array of perpendicularly magnetized dots can compensate the applied magnetic field and selectively enhance the critical field of the superconducting thin film for a given polarity [43,87,100,101]. This effect, which is also linked to the creation of vortex–antivortex pairs, can be optimized *in situ* by tuning the perpendicular magnetization of the dot array [102,103]. Also, a maximum in the critical current for nonzero applied field or field polarity dependent flux creep have been reported [104].

3.4. Size effects: with dot diameter

Generally, the defect size plays an important role in the periodic pinning as shown in Fig. 3. More minima appear in the magnetoresistance (or maxima in the critical current) as the dot diameter d increases, indicating an enhanced pinning [49].

This is caused by the two parameters which increase with dot size: the magnetic moment (proportional to dot volume) and area πd^2 (i.e. the area in the superconductor with reduced superconductivity due to the stray field or proximity effect). With increasing moment, multiple flux quanta are induced by the magnetic field of the dot [73,80], as mentioned above, and with a larger area, more than one vortex is pinned at each defect, as observed in superconducting films with arrays of antidots [105–107]. The maximum number of vortices ("saturation number" n_s) pinned by an insulating inclusion of diameter d is given by [108] $n_s = d/4\xi(T)$, where $\xi(T)$ is the superconducting coherence length. Fig. 3 shows n_s calculated for $\xi = 58$ and 33 nm (solid and dashed lines), the limiting values of the coherence length for the temperature ranges included in this figure. However, the number of matching peaks in the magnetoresistance of Nb films with arrays of magnetic dots usually exceeds considerably this saturation number [49], indicating that, in the higher order matching fields, multiple strongly pinned vortices at the magnetic dots coexist with weakly pinned interstitial ones [66,105,109,110]. Molecular dynamics simulations in the London limit [111] show that, the critical current peaks (minima in the magnetoresistance curves) are of similar magnitude at different matching fields for multivortex pinning, whereas for individual vortex pinning a sharp drop in the critical current at the matching conditions occurs once interstitial vortices appear in the superconductor. Another signature of the coexistence of strongly pinned vortices at the periodic defects with weakly pinned interstitial vortices at the higher matching fields, is a change in the I–V curve shapes, with an enhanced dissipation at low currents due to the motion of interstitial vortices and a kink at higher currents when the vortices at the periodic pinning centers become depinned [112]. These two effects allow discriminating experimentally between individual and multiple vortex pinning at the higher matching fields [49].

3.5. Size effects: interdot separation

Another important geometrical parameter changing with dot diameter is the dot edge-to-edge separation $s = a - d$. Fig. 4 shows a comparison between two samples with (600 nm × 600 nm) arrays of dots but different dot size: $d = 400$ nm (upper curve) and 530 nm (lower curve) [49] Although the dot diameter is only 25% larger in the lower curve, the number of minima has increased from 3 to 35. On the other hand, the dot separation has decreased considerably from $s = 200$ nm (upper curve) to 70 nm (lower curve). This is comparable to the superconducting coherence length $\xi(T)\sim 60$ nm, i.e. of the order of dot separation in the lower curve. In fact, independent measurements in samples with similar sized dots d but different separation s (i.e. different square lattice parameter a) unambiguously show [49] a crossover in the pinning behavior when the edge-to-edge distance becomes comparable to the superconducting coherence length. In this case, the number of resistivity minima is greatly enhanced, maxima appear in the critical current that were not present in the weak pinning regime and the resistivity anomalies at matching $\Delta\rho/\rho$ become a monotonous decreasingly function of current and field.

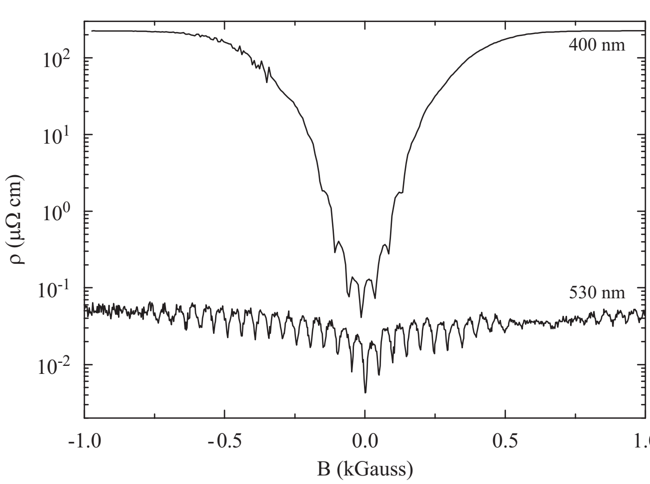

Fig. 4. Magnetoresistance curves for 100 nm thick Nb films with (600 nm × 600 nm) square arrays of Ni dots with dot diameter $d = 400$ nm (top curve) and $d = 530$ nm (bottom curve). The curve for the 400-nm Ni dots is shifted by a factor of 10 for clarity (after Hoffmann et al. [49]).

For small magnetic dot separation, the pinning potential wells overlap, so that the distances between the magnetic dots are too small to accommodate a vortex. Thus, the sample no longer behaves as a continuous film with a periodic array of pinning centers, but more like a superconducting wire network [113], and the magnetoresistance minima are caused by periodic quantization similar to the Little-Parks oscillations [113,114]. This is also found in superconducting films with antidot lattices when the interhole distance becomes comparable to $\xi(T)$ [105,115]. Furthermore, this crossover has been theoretically studied using nonlinear Ginzburg–Landau theory [116].

3.6. Magnetic antidots

The limiting case for decreasing dot separation corresponds to $s = 0$, when the magnetic dots physically touch. This limit corresponds to a qualitative change in the magnetic nanostructure, which instead of being composed of individual magnetic dots, becomes a continuous magnetic film with an array of holes or "antidots". In these patterned magnetic films, periodic magnetic closure domains appear with domain walls pinned at the antidots and governed by the array geometry [117–120]. Vortex pinning may arise due to the stray field produced by the domain structure in the magnetic material, as observed in continuous superconducting/ferromagnet bilayers [74,121–123].

Two different types of experiments were performed regarding this kind of systems: in the first [124,125], a superconducting Pb film was deposited on top of a perpendicular anisotropy Co/Pt multilayer with a square array of antidots. The magnetization curves of the superconducting film show periodic pinning effects after the magnetic film has been magnetized out of plane so that the stray field pattern (measured by magnetic force microscopy) is localized at the antidots. This periodic pinning is strongly asymmetric with respect to the field polarity, similarly to the arrays of out-of-plane magnetized dots [30,52]. Furthermore, matching is considerably reduced in the demagnetized state of the Co/Pt multilayer that presents an irregular domain structure [125] indicating a predominantly magnetic contribution to the pinning potential.

A second class of experiments corresponds to a superconducting film deposited on top of a nanostructured Co film with strong in-plane anisotropy [126,127]. In this case, no matching effects were observed in the magnetization curves of the superconducting layer, but only an overall enhancement of the critical current after the sample was magnetized along an in-plane easy axis in comparison with the demagnetized state. This effect was attributed to pinning of the vortex lattice by the network of domain walls emanating from the antidots, instead of the periodically arranged antidots.

4. Distorted arrays of magnetic dots: rectangular

4.1. Vortex-lattice reconfiguration

As discussed in the previous section, one of the first observations in the study of pinning effects by periodic arrays of pinning centers was that a square array of pinning centers is able to stabilize a square vortex lattice [15], although the preferred vortex configuration in a homogeneous superconducting film would be a triangular lattice induced by the inter-vortex repulsive interactions [26]. The vortex lattice is very sensitive to perturbations and many different vortex phases have been described [2,128] depending on the balance between different energy terms such as the pinning potential landscape, vortex-lattice elastic energy, thermal fluctuations and driving force. For a square array of pinning centers for example, the transition between square and distorted triangular vortex-lattice phases has been theoretically studied as a function of the strength of the periodic pinning potential [59].

For lower symmetry pinning arrays, such as rectangular arrays of circular magnetic dots, the balance between elastic and pinning energies has a more profound impact on the magnetotransport properties of the superconducting film. Fig. 5 shows ρ vs. B for a Nb film with a 400 nm × 625 nm rectangular array of Ni dots [32] at $0.97T_C$ with the transport current applied parallel to the long side of the rectangular array cell. Periodic dissipation minima appear, in a similar way as in samples with square arrays of pinning centers but, in this case, two different field regimes can be clearly identified. At low fields, the minima are sharp with spacing $\Delta B_{\mathrm{low}} = 81$ G, that corresponds well with the matching field calculated for a rectangular vortex lattice with one vortex per array cell $B_1^{\mathrm{rect}} = \Phi_0/ab = 83$ G. However, at high fields (beyond approximately 300 G), the dissipation minima become broader and their spacing increases to $\Delta B_{\mathrm{high}} = 112$ G, which is close to the matching field of a square vortex lattice of parameter $a = 400$ nm, $B_1^{\mathrm{sq}} = \Phi_0/a^2 = 129$ G. Thus, at low fields, the vortex lattice is distorted by the strong pinning potential into a rectangular configuration that matches the Ni dot rectangular array $a \times b$ cell, whereas at high fields vortex–vortex interactions become dominant and there is a reconfiguration transition in the vortex lattice, which adopts a more symmetric square configuration that is only matched along the short side of the rectangular array cell a corresponding to the direction of vortex motion.

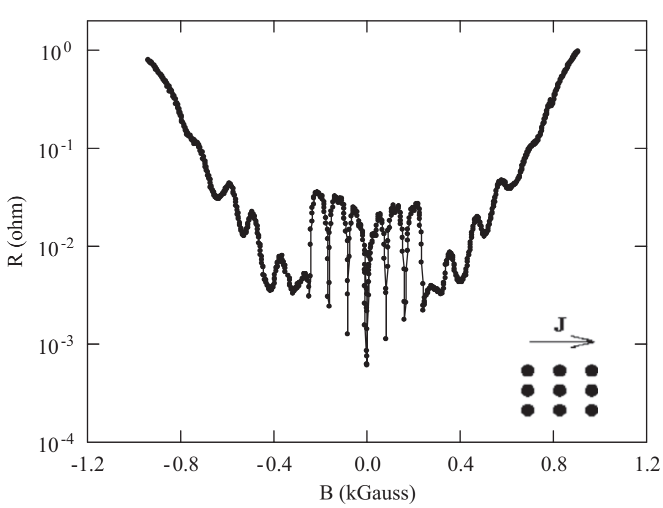

Fig. 5. Magnetoresistance curve for a 100 nm thick Nb film with a (400 nm × 625 nm) rectangular array of Ni dots at $0.97T_C$ and $J = 2.5 \times 10^4$ A/cm^2. Also shown is a schematic of the current configuration with respect to the dot array (after Martin et al. [32]).

The equilibrium vortex-lattice configurations, induced by the interaction with a rectangular array of pinning centers with $b/a = 2$, have been theoretically studied [129] for logarithmically interacting Pearl vortices for up to nine vortices per unit cell of the array. At low fields, the vortex configurations present rectangular symmetry (for the first two matching fields), and as the vortex density increases different, more symmetric lattices are stabilized (square, distorted triangular, and disordered). This gives rise to a crossover in the pinning behavior described in terms of the critical current anisotropy and the sharpness of the matching peaks [129].

The vortex-lattice ground states have also been analyzed using geometrical arguments (maximizing the shortest intervortex distance in order to minimize the intervortex repulsive interactions) for different values of the rectangular array aspect ratio b/a [130]. Ordered configurations are found not only for integer matching fields, but also for fractional fillings of the rectangular array unit cell, in agreement with the experimental observation [131].

Besides the differences in matching fields, there are several other changes in the magnetotransport properties at the reconfiguration transition: at low fields, $\rho(B)$ is almost independent of the measurement current [32] and matching peaks are also observed in the critical current [53]; however, at high fields, periodic pinning is only observed in an optimal current range, indicating that dynamic ordering in the vortex lattice is much more important in this second regime [32]. Also, at low fields, the angular dependence of the magnetoresistance curves can be simply scaled using the normal component of the magnetic field, whereas dissipation increases significantly as the field deviates from the film normal in the high-field regime [131].

The location of the crossover field between the low- and high-field regimes has been found to be weakly temperature dependent [53] and there is weak hysteresis depending on the direction of the field ramp [131]. In a first approximation, the field position of the reconfiguration transition can be estimated in terms of the balance between the extra elastic energy ΔE_{el} stored in the rectangular vortex lattice and the pinning energy gained by perfect matching $\Delta E_{\mathrm{P}} = \varepsilon_{\mathrm{P}}/ab$. This provides an estimate of the pinning energy per Ni dot in a 100 nm thick Nb fil, $\varepsilon_{\mathrm{P}} = 10^{-12}$ erg [32]. This energy is close to the superconducting condensation energy in the volume just above the Ni dot, indicating that destruction of superconductivity by the proximity effect plays a major role [132].

A similar reconfiguration transition from low-field rectangular vortex lattice to high-field square has been observed in Nb films grown on a Si substrate with a rectangular array of indentations [133] (i.e. nonmagnetic artificial defects). However, in this case, the reconfiguration field was significantly smaller than in a sample with a rectangular array of Ni dots of similar geometrical dimensions. This indicates again a reinforced pinning in the case of the magnetic dots in comparison with nonmagnetic defects [133], in good agreement with the observations in samples with square arrays of dots [49]. Also, the reconfiguration transition has been analyzed in Nb samples with rectangular arrays of 30 nm thick Ni dots covered with a variable thickness Ag layer (0–9.5 nm) [134]. In this way, both the corrugation induced by the Ni dot array and the interfacial proximity effect between the magnetic material and the Nb film could be varied. However, the presence of the Ag layer was found to have very little effect on the periodic pinning [134] implying that the pinning has an important magnetic contribution, although corrugation effects are substantial.

4.2. Anisotropy in the current direction

Besides the reconfiguration transition, the anisotropy in the periodic pinning as a function of the direction of motion of the vortex lattice relative to the array may play an important role. This anisotropy can be controlled by the applied transport current **J** that induces a Lorentz force on the vortex lattice given by $\mathbf{F}_L = \mathbf{J} \times \mathbf{B}$. For a magnetic field perpendicular to the sample plane (i.e. along z) $\mathbf{F}_L$ is always in the sample plane, at right angles to the transport current. In magnetotransport measurements the applied current direction is defined by the Nb bridge geometry. In a number of experiments, the relative angle between the applied current and the rectangular array is varied changing the shape of the Nb bridge [135–137]. For example, Fig. 6(a) shows a cross-shaped measurement bridge [136,138] that allows varying in a continuous fashion the angle θ between the Lorentz force and the short side of the array cell from 0° to 90° (see sketch in Fig. 6(b)). This is accomplished by the combination of applied currents along a and b (J_a and J_b respectively). Also indicated in Fig. 6(b) is the angle α that defines the direction of motion of the vortex lattice relative to the rectangular cell. In order to fix the notation, in the discussion below $b > a$ will always be assumed.

Fig. 7 shows the magnetoresistance of a Nb film on top of a 400 nm × 500 nm rectangular array of Ni dots with the transport current along the long and short sides of the rectangular array cell (i.e. $\theta = 0°$, solid symbols and $\theta = 90°$, open symbols) [139]. The same matching field is found in both directions caused by the commensuration condition of one vortex per unit cell, as shown previously. However, a clear anisotropy appears in the background dissipation at low fields (i.e. away from the matching conditions): the resistivity is much lower for $\theta = 90°$, i.e. when the vortex lattice moves along the long side of the array cell, than for $\theta = 0°$, i.e. when the vortex lattice moves along the short side of the array cell.

This behavior has been predicted [129] by numerical simulations that indicate that a rectangular array of pinning centers induces an easy direction of motion for the vortex lattice along the short side of the array cell. In this case, there is a clear signature of the periodic pinning. On the other hand, for vortex motion along the long side, the pinning force is higher both at matching and elsewhere. Since in this case the pinning values are similar this results in the overall reduction of dissipation, together with less pronounced matching effects as observed in Fig. 7.

A similar critical current anisotropy was observed in magnetooptical images of the flux penetration in Nb and $YBa_2Cu_3O_7$ films with a rectangular array of antidots [140,141]. In these experiments, vortices are found to penetrate preferentially in the sample along the antidot rows, i.e. along the short side of the antidot array a. Thus, an anisotropic critical state is established,

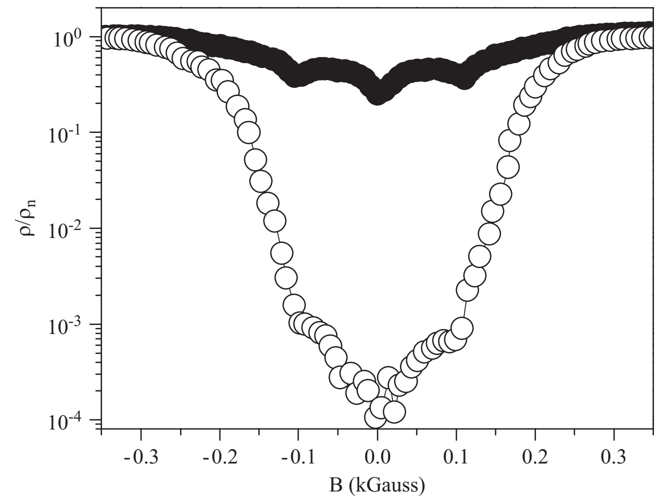

Fig. 7. Magnetoresistance curves for a 100 nm thick Nb film with a (400 nm × 500 nm) rectangular array of Ni dots measured at $T = 0.995T_C$ with $J = 1.25 \times 10^4\,\mathrm{A\,cm^{-2}}$ with different Lorentz force directions relative to the array: $\theta = 0°$, solid symbols; $\theta = 90°$, open symbols (after Villegas [139]).

which is characterized by a lower critical current along a than along b.

4.3. Size effects in rectangular lattices: the channelling regime

As found earlier for the square arrays of magnetic dots, a change in pinning can be expected when the dot size is increased, so that interdot separation becomes comparable with the superconducting coherence length and the potential wells produced by individual dots start to overlap. However, in rectangular arrays of circular dots, interdot separation along a and along b will be very different so that this overlap of potential wells occurs first only along a, the short side of the array cell.

Fig. 8 shows $\rho(B)$ for a Nb film with a 350 nm × 500 nm array of Ni dots of diameter $d = 230$ nm and interdot separations $s_a = 120$ nm and $s_b = 270$ nm at $T = 0.99T_C$ for two perpendicular directions of vortex motion: $\theta = 0°$, Fig. 8(a) and $\theta = 90°$, Fig. 8(b) [135]. At this temperature, the coherence length estimated from the temperature dependence of the upper critical field $\xi = 114$ nm, close to s_a. Once again, the overall resistivity values are an order of magnitude lower for $\theta = 90°$ than for $\theta = 0°$ but, now, the spacing between minima also changes with the vortex motion direction. In Fig. 8(a), the matching field is $B_1^{0°} = 120$ G, which agrees very well with the calculated value for one vortex per unit cell of the rectangular array $B_1^{\mathrm{rect}} = \Phi_0/ab = 118$ G. However, $\rho(B)$ in Fig. 8(b) shows matching fields at $B_1^{90°} = 185$ G that corresponds to the matching field a triangular vortex lattice of parameter 360 nm, $B_1^{\mathrm{triang}} = (4/3)^{1/2}\,\Phi_0/a^2$.

This anisotropy in matching conditions (Fig. 7) cannot be understood in terms pinning by a rectangular array of weak pinning centers [129], because these would give similar matching fields for both current directions. When the distance s_a between individual dots along a becomes comparable to ξ, the pinning landscape consists of deep channels slightly modulated with a period a and spaced at a distance b [135] For motion along the potential channels ($\theta = 0°$), the vortex-lattice orders in one-dimensional (1D) lines inside the channels and matching effects appear when the vortices in each line match the small modulation of period a. This results in the same matching field $B_1^{\mathrm{rect}} = \Phi_0/ab$ as for a rectangular array of weak pinning centers. However, the reconfiguration transition would not be produced by a channelled landscape and indeed, has not been observed experimentally in

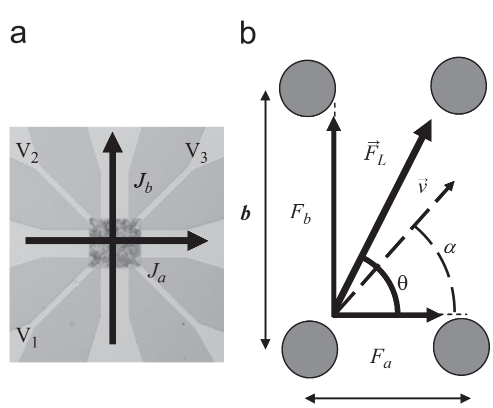

Fig. 6. (a) Micrograph of a cross-shaped Nb measurement bridge that allows to control the transport current direction. The shaded area represents the 90 × 90 μm² array of dots. (b) Definition of angles θ and α for the Lorentz force and vortex velocity directions relative to array axes (after Villegas et al. [138]).

samples with small s_a. On the other hand, the vortex correlations, for motion in the hard direction across the channels ($\theta = 90^\circ$), are hindered by disorder whereas *transverse* order persists [128,142]. A similar loss in *longitudinal* order with persistence of long-range *transverse* order was also found in numerical simulations for periodic potentials [143]. Thus, for $\theta = 90^\circ$, periodic pinning is observed when the density of vortices inside each channel matches the lattice parameter of the Ni dot array perpendicular to the motion (i.e. along *a* in this case).

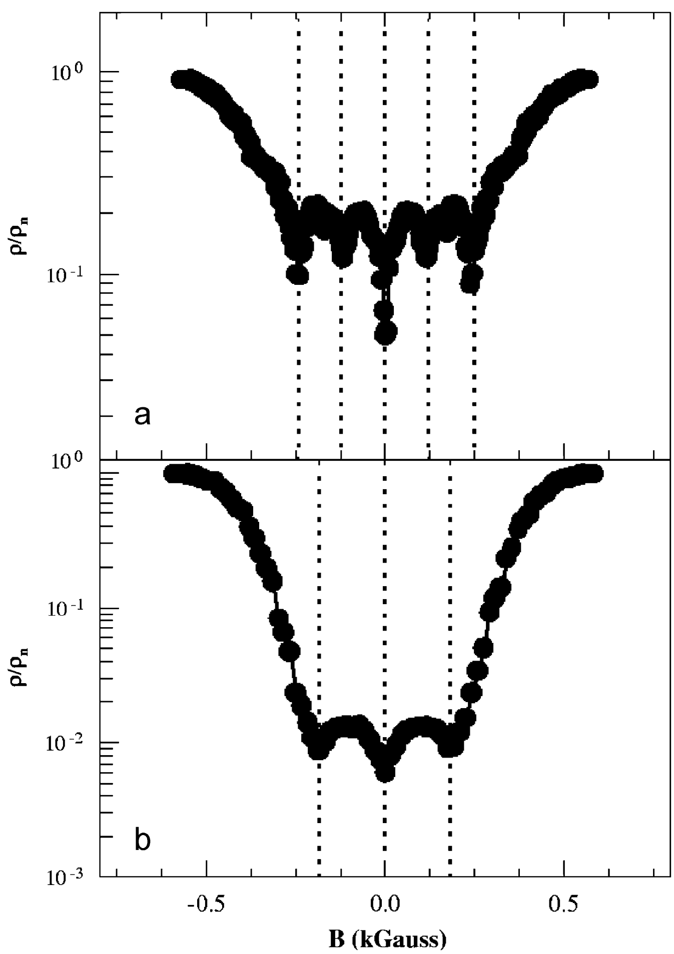

Fig. 8. Magnetoresistance curves for a 100 nm thick Nb film with a (350 nm × 500 nm) rectangular array of Ni dots of diameter $d = 230$ nm and interdot separations $s_a = 120$ nm and $s_b = 270$ nm measured at $T = 0.99T_C$ with $J = 3.7 \times 10^3$ A cm^{-2} for two perpendicular Lorentz force directions: (a) $\theta = 0^\circ$; (b) $\theta = 90^\circ$ (after Vélez

4.4. Guided vortex motion by the anisotropic pinning landscape

Generally, periodic pinning arrays exhibit anisotropy in the pinning landscape with easy and hard directions for vortex motion connected to the symmetry directions of the array. Theoretical work on different systems with square pinning potentials [61,144–146] has shown the possibility of guided vortex motion along the principal axes and diagonals of the arrays. This effect has been observed experimentally in a limited angular range for superconducting films with square arrays of antidotes [147]. Thus, rectangular arrays of magnetic dots combining a strong pinning potential with low array symmetry provide an ideal system for the study of guided vortex motion with artificial mesoscopic pinning potentials [136,138].

The magnetoresistance for different applied current directions relative to the array cell (i.e. angle θ of the Lorentz force) shows a strong guiding effect [136]. The vortex motion is essentially confined along the short side of the array cell in a wide angular range from $\theta = 0^\circ$ to 85°. Fig. 9(a) [138] shows the angle α, the vortex-lattice direction of motion, as a function of the applied driving force direction θ for a Nb film with a 400 nm × 625 nm rectangular array of Ni dots (solid symbols) measured at the first matching field. The data for a Nb film with a 500 nm × 500 nm square array of Ni dots (open symbols) is also shown for comparison. For the square array, the vortex lattice moves essentially parallel to the applied driving force (i.e. $\alpha \approx \theta$). This can be attributed to the existence of two equivalent easy flow paths along the two sides of the square array. This way the vortices can follow the driving force direction moving in a staircase fashion switching from one easy path to the other. On the other hand, for the rectangular array, the motion direction is locked close to $\alpha = 0^\circ$ almost up to $\theta = 80^\circ$ and it only becomes parallel to the driving force for $\theta = 90^\circ$.

Hall effect measurements in samples with rectangular arrays of Ni dots have also shown evidence for guided vortex motion [137] in a wide angular range. Moreover, the analysis of flux penetration in superconducting films with rectangular arrays of holes indicates that vortices are guided by the antidot array, so that vortex motion in the critical state occurs only along either *a* or *b*, depending on which is closest to the Lorentz force direction [141].

The guided motion of the vortex lattice by a rectangular array of pinning centers can be characterized in terms of a transverse

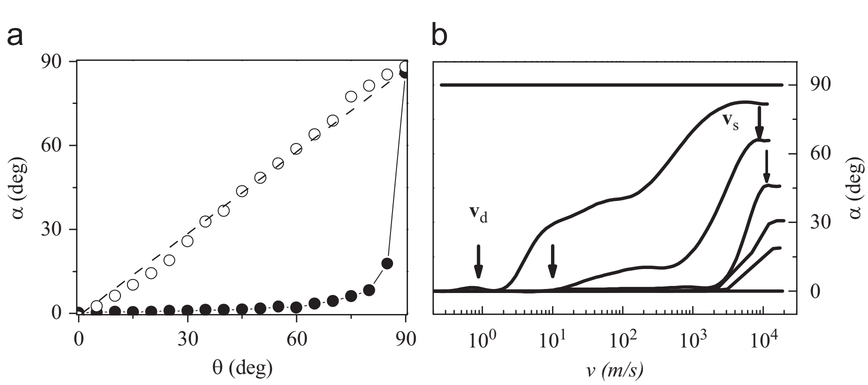

Fig. 9. (a) Vortex-lattice direction of motion $\alpha = \mathrm{arctag}(v_b/v_a)$ as a function of the direction of the driving force θ: solid symbols, Nb film with a (400 nm × 625 nm) rectangular array of Ni dots at $T = 0.99T_C$, $B = 84$ G (first matching field) and $F_L = 1.3 \times 10^{-7}$ N/m; open symbols, Nb film with a (500 nm × 500 nm) square array of Ni dots at $T = 0.995T_C$, $B = 82$ G (first matching field) and $F_L = 5.17 \times 10^{-7}$ N/m. (b) Vortex-lattice direction of motion α vs. its velocity $v = (v_a{}^2 + v_b{}^2)^{1/2}$ for several angles $\theta = 0^\circ$, 30°, 45°, 60°, 75°, 85°, and 90° (from bottom to top) for a Nb film with a (400 nm × 625 nm) rectangular array of Ni dots at $T = 0.99T_C$ and at the second matching field (after Villegas et al. [138]).

depinning force. This is illustrated by a plot [Fig. 9(b)] of α as a function of vortex velocity v for different applied driving force directions θ derived from current voltage characteristics at the second matching field for a Nb film with a 400 nm × 625 nm rectangular array of Ni dots [138]. Three regimes are found for each curve: for low velocities, the vortex motion is guided along the channels in the pinning landscape ($\alpha = 0°$); for intermediate drives the vortex lattice starts to depin in the transverse direction and α rotates towards θ and, finally, for large drives, the vortex lattice moves parallel to the driving force (i.e. $\alpha \approx \theta$). The transitions between these different regimes are governed by the dynamical evolution of order in the vortex lattice as a function of driving velocity.

4.5. Matching effects by periodic arrays of magnetic lines

As dot size increases beyond $d = a$, when the interdot separation along this side of the array vanishes, the magnetic dots touch and the rectangular array of pinning centers becomes a periodic array of magnetic lines. Thus the pinning potential changes from a 2D anisotropic landscape (in the case of rectangular arrays) to a set of equally spaced 1D channels.

Fig. 10 shows the magnetoresistance of a Nb film covering an array of Ni lines with period $b = 500$ nm and width $d = 200$ nm [148]. Fig. 10(a) corresponds to vortex motion perpendicular to the lines (i.e. $\theta = 90°$) and Fig. 10(b) to vortex motion along the lines direction (i.e. $\theta = 0°$). The overall resistivity anisotropy is similar to the case of rectangular arrays of Ni dots (Figs. 7 and 8) with a much lower dissipation for $\theta = 90°$ than for $\theta = 0°$, which can be attributed to the anisotropy in the channelled pinning landscape. Similarly, the critical current is found to be much larger for $\theta = 90°$ than for $\theta = 0°$ [148]. It is interesting to note that a similar critical current anisotropy has also been predicted for a superconducting/ferromagnetic bilayer with a 1D pinning potential created by a stripe domain structure in the ferromagnetic layer [149].

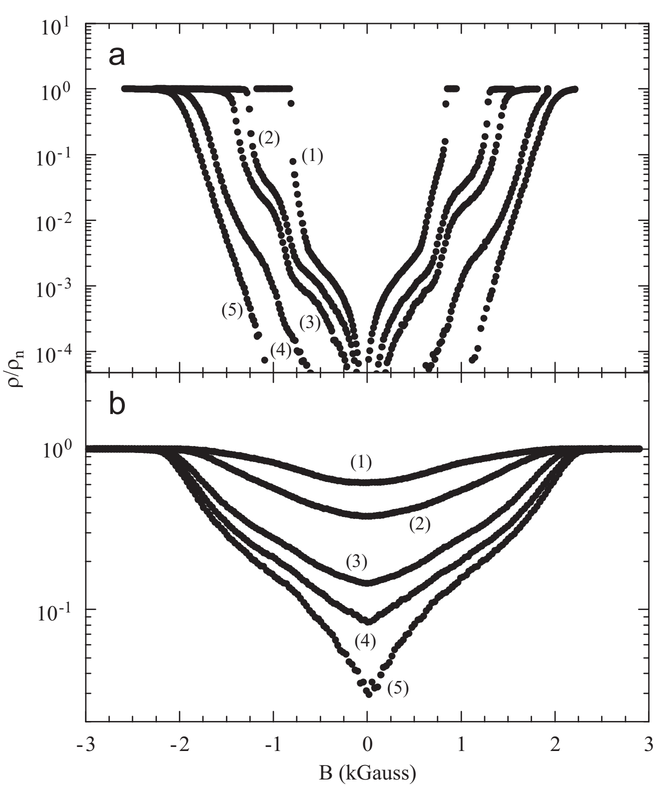

Fig. 10. Magnetoresistance curves for a Nb film with an array of 200 nm wide Ni lines with period $b = 500$ nm at $T = 0.94\,T_C$: (a) Lorentz force perpendicular to the lines ($\theta = 90°$): (1) $J = 2.2 \times 10^5$ A/cm^2; (2) $J = 1.2 \times 10^5$ A/cm^2; (3) $J = 8.7 \times 10^4$ A/cm^2; (4) $J = 5 \times 10^4$ A/cm^2; and (5) $J = 2.5 \times 10^4$ A/cm^2. (b) Lorentz force parallel to the lines ($\theta = 0°$): (1) $J = 5 \times 10^4$ A/cm^2; (2) $J = 2.5 \times 10^4$ A/cm^2; (3) $J = 1.2 \times 10^4$ A/cm^2; (4) $J = 8 \times 10^3$ A/cm^2; and (5) $J = 2 \times 10^3$ A/cm^2 (after Jaque et al. [148]).

However, the loss of periodicity along a in the line-geometry produces a marked change in the periodic pinning as shown in Fig. 10 [148]: in this case, no matching anomalies appear for $\theta = 0°$ whereas for $\theta = 90°$ plateaus at equidistant field intervals are observed in the $\rho(B)$, instead of the minima characteristic of pinning by the magnetic dot arrays. These matching plateaus are typical of pinning of a soft vortex lattice by 1D periodic potentials [150] such as superconducting/insulating superlattices. The matching field extracted from these plateaus in the magnetoresistance curves is $B_1 \approx 700$ G, which corresponds well with the matching field for a triangular vortex lattice of periodicity 190 nm, $B_1^{\text{triang}} = (4/3)^{1/2} \;\; \Phi_0/(200\,\text{nm})^2 = 660$ G. Thus, it appears that matching anomalies appear when intervortex distances match the Ni lines width ($d = 200$ nm) instead of the array periodicity (matching to $b = 500$ nm would give a much lower matching field of 95 G only). These results indicate, that for vortex motion along $\theta = 90°$, longitudinal correlations in the vortex lattice are smaller than the line period and that pinning occurs predominantly at the lines edges [148].

4.6. Phase diagram for square and rectangular arrays of magnetic dots

From the analysis of the different periodic pinning regimes described above, there are two geometrical parameters that appear to control the observed behavior: the aspect ratio of the array cell a/b, and the ratio between interdot separation and the superconducting coherence length $(a-d)/\xi$. The phase diagram shown in Fig. 11, summarizes the various pinning regimes observed experimentally in superconductors using arrays of magnetic dots as pinning centers. The axes correspond to parameters a and b of the array, expressed in units of the dot diameter d. The diagonal corresponds to the case of square lattices $a = b$ with four-fold symmetry, and the rest of the diagram to rectangular lattices with only two-fold symmetry in which a/b is smaller or greater than 1. Other important lines in the diagram correspond to: $a = d$ or $b = d$ that mark the limit when the dots are touching and, $a = d+\xi$ or $b = d+\xi$ that mark overlapping of pinning potentials between the individual dots (see schematics in Fig. 11).

Thus, the parameter space is divided into several regions (labelled A–F), that are symmetric along $a = b$ diagonal. In each, the interaction between the vortex lattice and the periodic potential created by the arrays of magnetic dots results in a different pinning behavior, characterized by a different matching field which can be calculated from the geometrical parameters of the array (see Table 1):

- Region A corresponds to the weak pinning of a square lattice with a matching field given by $B_1 = \Phi_0/a^2$ and a small number of matching anomalies.
- Region B is the ‘‘superconducting wire network’’ regime produced by a square lattice of dots with overlapping pinning potential wells. The matching field is again $B_1 = \Phi_0/a^2$ but a much larger number of matching peaks are observed up to the critical field.
- Region C corresponds to physically touching dots, i.e. a continuous magnetic film with a periodic array of antidots. Pinning is provided by the closure domain pattern and the domain walls in the magnetic film. Matching anomalies have only been observed for perpendicularly magnetized films in the remanent state.

- Region D corresponds to the weak pinning regime of rectangular arrays of magnetic dots. In this case, a low-field rectangular distortion of the vortex lattice is observed, indicated by a matching field $B_1^{\rm low} = \Phi_0/ab$. At high fields, the vortex lattice adopts a more symmetric square configuration characterized by a change in the matching field to $B_1^{\rm high} = \Phi_0/a^2$.
- Region E is the equivalent to Region B but with a lower symmetry and corresponds to the channelling regime in which pinning potentials overlap along the shortest array distance only. This is characterized by a different matching field depending on vortex motion relative to the potential channels, $B_1^{0^\circ} = \Phi_0/ab$ and $B_1^{90^\circ} = (4/3)^{1/2}\Phi_0/a^2$. In both regions D and E, clear guiding of the vortex motion along channels in the periodic pinning potential has been observed.
- Region F corresponds to the case of periodic arrays of magnetic lines. The most relevant characteristic of this regime is the strong critical current anisotropy between vortex motion parallel and perpendicular to the lines (similarly as in regions D and E). Matching anomalies only appear for vortex motion across the lines with $B_1 = (4/3)^{1/2}\ \Phi_0/d^2$ corresponding to matching to the linewidth.

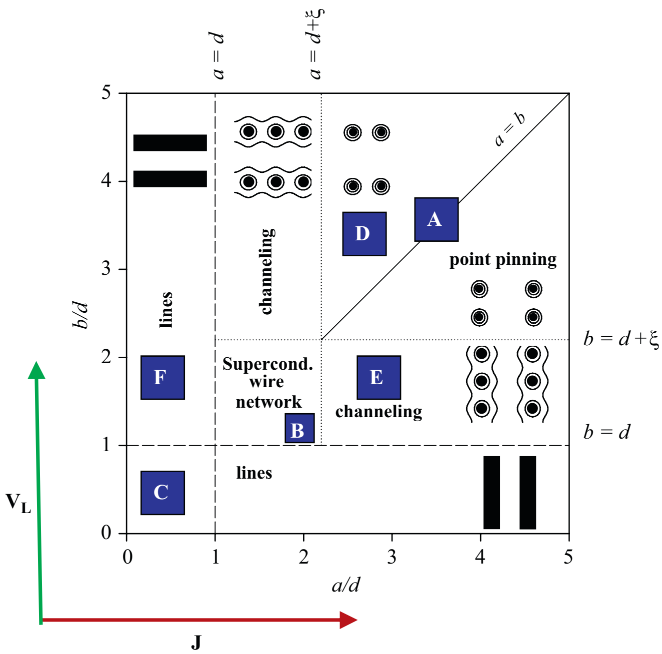

Fig. 11. Phase diagram for periodic vortex pinning with periodic square and rectangular arrays of magnetic dots as a function of array anisotropy and dot size. The different pinning regimes are discussed in the text.

5. Distorted arrays of magnetic dots: *asymmetric* and *aperiodic* pinning

So far we have discussed vortex dynamics and new phenomena that appear with periodic pinning arrays of magnetic dots, either regular (with six-fold (triangular) and four-fold (square) symmetry) or distorted with only two-fold (rectangular) symmetry. More recently, other types of *ordered* artificial pinning potentials with further reduced symmetry have been subject of research. Two systems are of particular interest: ordered arrays of asymmetric magnetic particles (e.g. triangular instead of circular) which provide a pinning potential with broken inversion symmetry and *quasiperiodic* arrays of magnetic dots. The former give rise to the so-called *vortex ratchet* effect; the latter may induce *quasiperiodic* order in the vortex lattice with unexpected long-range correlations, and implies enhanced critical currents. These effects illustrate dramatically to what extent the dynamic

Table 1
Summary of the different periodic pinning regimes and their corresponding matching fields induced by square and rectangular lattices of magnetic dots for the different ranges of geometrical parameters of the dot array

b	*d*		$\theta = 0^\circ$		$\theta = 90^\circ$	References
$b = a$ Square lattice	$a+\xi > d$	A. Point pinning	Φ_0/a^2 Small number of matching peaks			[30,31,40,42–44,48–53,57,62,64,104,111]
	$a > d > a+\xi$	B. Superconducting wire network	Φ_0/a^2 Large number of matching peaks			[49]
	$d > a$	C. Patterned magnetic film	Out of plane	Matching to closure domain pattern		[124,125]
			In plane	Pinning by domain walls		[126,127]
$b > a$ Rectangular lattice	$a+\xi > d$	D. Point pinning	Low B	High B	Φ_0/ab	[32,53,131,133,134,139]
			Φ_0/ab	Φ_0/a^2		
	$a > d > a+\xi$	E. Channeling	Φ_0/ab		$(4/3)^{1/2}\Phi_0/a^2$	[135–138]
	$d > a$	F. Lines	No matching		$(4/3)^{1/2}\Phi_0/d^2$	[148]

References correspond to the experimental observation of the different regimes.

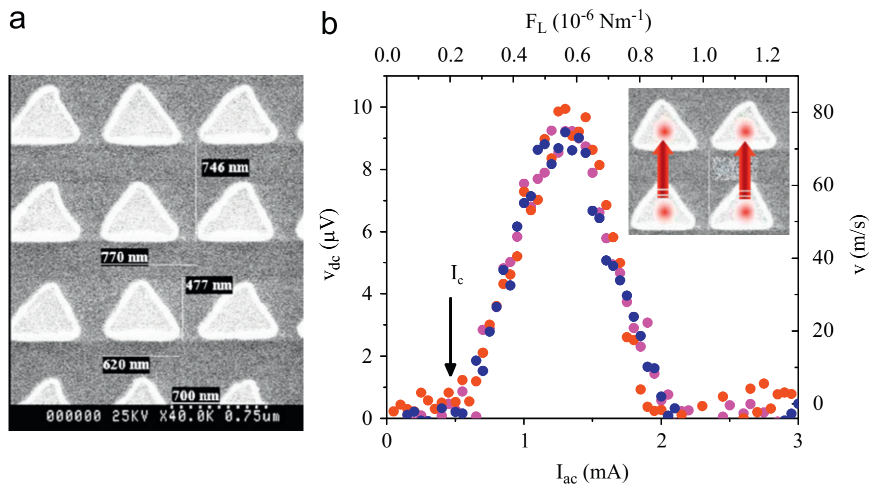

Fig. 12. (a) Scanning electron microscopy image of an array of Ni nanotriangles. (b) DC voltage V_{DC} (proportional to the average net velocity v of the vortex lattice) as a function of the injected AC current amplitude I_{AC} (that give an AC Lorentz force of amplitude F_L) for different AC frequencies $\omega = 10\,\mathrm{kHz}$, $\omega = 1\,\mathrm{kHz}$, and $\omega = 0.5\,\mathrm{kHz}$ (magenta, blue an red circles, respectively) measured in a 100 nm thick Nb film deposited on top of the array of triangles shown in (a), at $T = 0.99T_C$ and with an applied field $B_1 = 32$ Gauss (first matching field, see cartoon in the inset) (after Villegas et al. [35]).

and static properties of the vortex lattices can be manipulated using ordered arrays of pinning centers. We briefly review below some of the studies that deal with those effects.

5.1. *Asymmetric pinning*

Asymmetric pinning potentials are able to rectify AC driving forces, leading to a new type of controlled vortex motion in which the vortex lattice acquires a net velocity out of an unbiased (zero time-averaged) alternate drive. This so-called "ratchet effect" [151] constitutes a unique model system in which nonequilibrium properties of the vortex lattice can be investigated. Interestingly, this effect has broad implications in many other fields within Physics and Natural Sciences, which span from biological motors [152] to Brownian motion [153].

Vortex ratchets were first investigated theoretically [154–160] and, experimentally realized using asymmetric magnetic pinning centers [35,36]. Fig. 12 shows the essential phenomenology, observed in a superconducting Nb thin film with periodic arrays of magnetic (Ni) nanotriangles (Fig. 12(a)). As discussed above, application of a magnetic field B_1 ("matching" field) perpendicular to the film plane leads to a situation in which there is one vortex per magnetic pinning site in the array (inset of Fig. 12(b)). If an AC electrical current of amplitude I_{AC} is injected *in-plane* along the base of the triangles, an AC Lorentz force F_L is exerted on the vortices, which points in the perpendicular direction. The pinning potential with broken inversion symmetry along this direction produced by the *asymmetric* shape of the pinning sites rectifies the vortex motion: i.e. when the AC current amplitude (Lorentz force) exceeds a critical value I_c the lattice is pushed back and forth and therefore the vortex motion is easier in one direction (say forward). Thus, the vortices acquire a net drift velocity (forward) out of a zero-averaged AC drive. This drift velocity (which is experimentally detected as a DC voltage V_{DC}) first increases as the amplitude of the AC drive is increased, until a maximum is reached (see Fig. 12(b)). Further increase of the AC drive amplitude results in a decrease of V_{DC}, and finally the effect vanishes completely in the same way as is observed for vortex motion in symmetric potentials [62].

This vortex ratchet effect has attracted much attention recently. In addition to the above-described system, vortex ratchets have been experimentally realized in films with asymmetric arrangements of "antidots" [161,162], square arrays of Cu nanotriangles [163], Josephson junctions arrays [164], superconducting constrictions (induced by surface-barrier effects) [165], asymmetric pinning produced with ion irradiation [166], magnetized strips [167] or spacing-graded arrays of pinning centers [168], in asymmetric-shaped mesoscopic superconductors [169], and in films with arrays of magnetic dipoles [170,171]. The phenomenology observed in these systems is very rich. It is remarkable for instance that in some of them [35,36,162,166,172] the ratchet effect is reversible (i.e. the sense of net vortex motion or *drift* is reversed) depending on the density of the vortex lattice, which is controlled by an external parameter (e.g. the applied magnetic field). The origin of the ratchet reversal is a very active research field, and different scenarios have been reported, for instance interplay between interstitial and pinned vortices [35,36,162,166], vortex-lattice reconfiguration [173], interplay between the superconducting characteristic lengths and the period of the asymmetric potentials [174], or vortex lattice instability [175]. Interestingly, these ratchet reversal mechanisms are common to general systems of interacting particles [176]. More subtle effects such as "transverse" rectification (in the direction perpendicular to the driving force) have been also explored theoretically [177] and experimentally [178]. Finally, a different type of vortex ratchets have been recently realized in high-T_C superconductors, induced by time-asymmetric drives [179] instead of spatially asymmetric pinning.

5.2. *Quasiperiodic and fractal pinning*

As discussed in Section 3, the interaction between the vortex lattice and periodic arrays of pinning centers is stronger for particular, well-defined vortex densities, for which commensurability ("geometrical matching") develops between the vortex lattice and the array. These matching effects are critical, i.e. appear as very sharp peaks (minima in the flux flow resistance or maxima in the critical current, as opposed to plateaus) as a function of the applied field. This suggests collective vortex pinning and implies a high degree of order with long vortex-lattice correlation lengths. However, commensurability effects between the vortex lattice with arrays lacking *periodic* order (*quasiperiodic* and *fractal* arrays) have been recently observed, implying in some cases that local order is sufficient to induce critical matching. We review below some of the most recent related studies.

Frustration in *quasiperiodic* and *fractal* superconducting networks was investigated earlier [180,181], but it was not until recently that commensurability between Abrikosov vortex lattices and *quasiperiodic* pinning potentials were studied theoretically [182] and experimentally [33,34,183]. Numerical simulations predicted commensurate states of the vortex lattice on one-dimensional (1D) Fibonacci chains and Penrose lattices [182], which manifest as peaks in the field dependence of the critical depinning current. Interestingly, these results predicted that enhanced pinning at well defined matching fields may originate from local commensurability between the vortex lattice and *quasiperiodic* arrays. This was also found in experiments on Nb thin films with 2D Fibonacci arrays of magnetic dots [33,34]. In these, commensurability originates from local matching situations repeated a number of times over the array, and do not imply long vortex-lattice correlations. Experiments on Nb thin films arrays of holes [183] and Pb and Al films with arrays of magnetic dots [34] confirmed the predictions from numerical simulations for Penrose lattices [182]. In addition [183], the background pinning (at fields different from matching) from Penrose arrays exceeds that from similarly dense *periodic* and disordered arrays of defects, as well as from the intrinsic defects in the films. Thus, these *quasiperiodic* arrays may be a useful avenue to increase critical currents *in a broad range of applied fields*.

A very striking behavior is observed in films with *quasiperiodic fractal* arrays [33], as the one shown in Fig. 13. This pentagonal array is self-similar at all length scales and shows inflation symmetry, and thus it has some similarities with periodic arrays. Interestingly, the magnetoresistance shows deep minima (comparable to those in periodic arrays), as well as a very rich fine structure [Fig. 13(b)]. The *quasiperiodic* series of minima implies that the lattice adopts the pentagonal symmetry of the array at different length scales. The long period magnetoresistance oscillations imply matching to the array geometry over the length scale of the interdot distance [smaller (blue) pentagons in Fig. 13(a)], while the shorter period corresponds to commensurability over longer length scales [that of the larger (red) pentagons in Fig. 13(a), and self-similar scaled-up units in the array]. These results imply that a *quasiperiodic* fractal vortex lattice is stabilized with remarkably long correlations, even if the lattice distortion with respect to its natural *periodic* order must have an adverse increase of elastic energy. Further theoretical work is needed to understand this unexpected behavior.

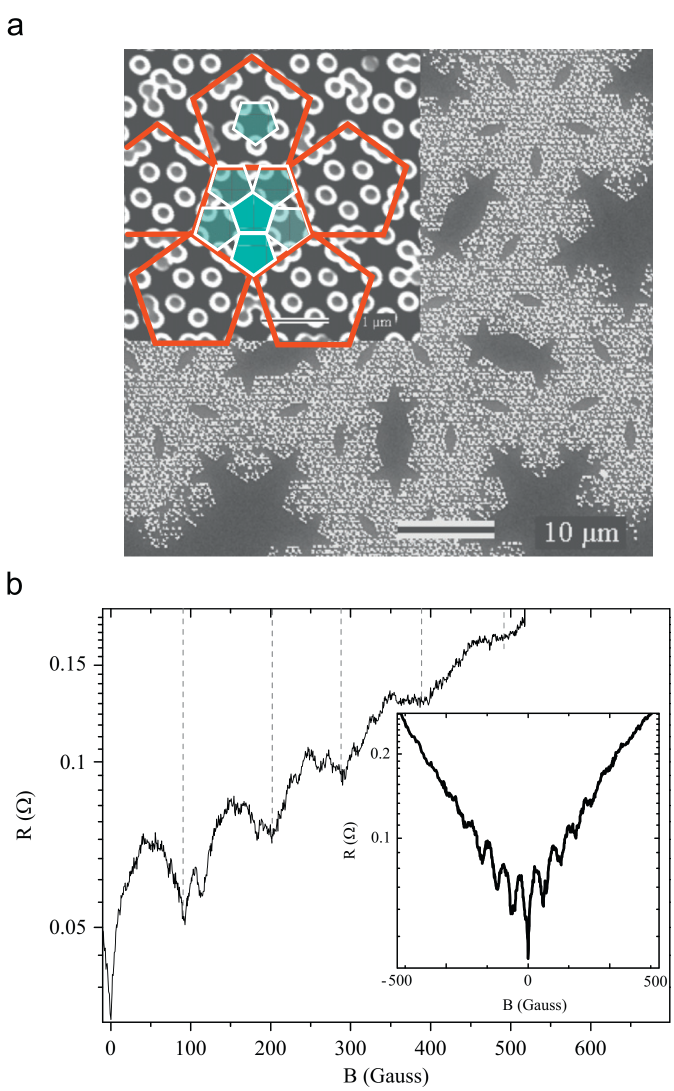

Fig. 13. (a) Scanning electron microscopy image of a pentagonal fractal *quasiperiodic* array of Ni dots. The inset shows a higher magnification image where self-similar pentagons are highlighted (blue and red). (b) Magnetoresistance of a 100 nm thick Nb film on top of the array shown in (a), at $T = 0.985T_c$ and $J = 1.5\,\mathrm{kA\,cm^{-2}}$. Vertical lines mark main minima. Inset: same curve as in (a) zoomed out (after Villegas et al. [33]).

6. Future outlook

Although much was done, as outlined above, this field is extremely rich in possibilities. Many opportunities are available and should produce interesting new results since all the relevant parameters can be controlled at will. Here, we will outline a few examples of possible research directions, which are expected to produce new and interesting physics.

6.1. Order– disorder effects in the vortex lattice

The interaction between the vortex lattice and periodic arrays of pining centers is stronger (leading to enhanced critical currents) for well-defined vortex densities. For these, commensurability develops between the vortex lattice and the array implying a high degree of order with long vortex-lattice correlation lengths. However, as reviewed in Section 5.2, commensurability effects have also been observed on arrays with only local order but lacking periodic order (quasiperiodic [33,34,182–184] and fractal arrays [33]) and with nonperiodic long-range order [33]. Moreover, matching effects have been recently observed in some systems with only short-range periodic pinning [185]. Clearly, further investigation is needed to clarify this confusing situation. Besides the particular interest within vortex physics, this issue is relevant for a variety of physical systems that span from epitaxy [186], to the physics of colloids [187] or other elastic media on fixed periodic potentials [142], for which vortex lattices on artificial pinning constitute a model system where to investigate the general problem of commensurability. Compared with these other physical systems, superconducting vortex lattices have the advantage that their density can be manipulated readily and reversibly via the external magnetic fields.

Thus, the crucial, largely unexplored question for all types of matching phenomena is how robust such commensurate states are against the introduction of disorder in the pinning array. This disorder can be structural (i.e. in the geometry of the pinning structures), magnetic (in the magnetic history of the pinning dots) or even dynamical (due to the effect of externally applied noise of various types).

6.2. Nonequilibrium effects in the vortex lattice and asymmetric pinning

As reviewed in Section 5.1, certain types of asymmetric pinning potentials are able to rectify AC driving forces, leading to a new type of controlled vortex motion in which the vortex lattice acquires a net velocity driven by an unbiased (zero time-averaged) alternate drive [35,36,162,164–166,172,179,188–190]. This so-called "ratchet effect" offers a unique system in which nonequilibrium properties of the vortex lattice can be investigated. Interestingly, in some systems the ratchet effect changes sign as the applied field increases [35,172], i.e. the effective asymmetry of the pinning potential depends on the vortex-lattice density. Some models explain this behavior in terms of the opposite asymmetry felt by a probe vortex depending on its position with respect to the asymmetric pinning centers (interstitial or directly on top of them) [35,176,191]. Others conclude that the whole lattice moves coherently and the sign change in the rectification arises from a vortex-lattice re-orientation as its density is changed [173,175]. This issue could be investigated by changing the geometry of the array of asymmetric pinning centers in a controlled way, to favor certain lattice rotations (or alternatively interstitial vortex distributions). This will allow identifying the origin of the observed vortex density-dependent rectification.

A worthwhile avenue of research is the preparation of ratchet potentials induced by "surface barriers" [165,189], as opposed to inducing them with asymmetric pinning centers distributed within the bulk of superconductors. It is well known that the entrance/exit of vortices in a superconducting film is governed by different surface barriers (such as Bean–Livingston or geometric barriers [192]). It is expected that vortex dynamics in narrow superconducting constrictions (a few times λ) will be dominated by such surface effects. Thus, simple ratchets could be obtained by manufacturing a narrow strip with differing surfaces (for instance crooked vs. sharp edges).

Finally, an interesting issue that has just began to be explored is the influence of the magnetic state of the asymmetric pinning centers [37,38,171] on the ratchet effect. This could provide a good tool to adjust the strength of the asymmetric potential in a single sample.

6.3. Frequency dependence of periodic pinning

A very important consequence of the interaction between the vortices and ordered potentials is the occurrence of collective pinning of the entire vortex lattice, implying coherent motion of the lattice as a whole [25]. An issue that remains unexplored is how robust is this coherent motion against the effect of high-frequency drives. For appropriate combinations of AC drive amplitude and frequency vortices would oscillate within their pinning potential wells, while for some others they would be able to hop from pinning site to pinning site within the period of the oscillation. If different vortices in the lattice are subject to different pinning strengths (for instance, vortices directly on the pinning sites or in interstitial sites [112]) the binding potential wells might be different. Consequently, if they are forced to oscillate by AC drives, one may expect regimes in which some vortices would remain pinned while others would depin. This may lead to a situation in which the lattice breaks into two sublattices as a function of the frequency of the AC drive. Moreover, this effect may be enhanced by the presence of different resonant frequencies for different vortices in the lattice, depending upon their position with respect to the pinning array. An ideal technique to perform this experiment, in addition to AC magnetotransport, is frequency-dependent AC susceptibility [193].

6.4. Periodic magnetic pinning in confined geometries

Boundary conditions play a major role in condensed matter physics in general and in particular in mesoscopic superconducting structures whose sizes are a few times the relevant length scales ξ and λ. Research in mesoscopic superconducting disks has shown that confinement induces dramatic effects on the vortex matter [194–198]. Changes may appear in the vortex phase transitions [199,200] and vortex-lattice geometry, for instance "rings "or "shells" as opposed to the usual triangular Abrikosov lattice. Moreover, theoretical studies predict that a magnetic nanodot on top of a mesoscopic superconductor can enhance superconductivity in hybrid structures [201] and can enforce or even induce symmetry-consistent vortex–antivortex molecules [202,203]. These predictions have been recently confirmed experimentally [204].

Therefore, a number of opportunities exist in the research of mesoscopic superconductors (disk or strips of sizes a few times the superconducting ξ and λ) with different types of ordered arrays of pinning centers. Investigating the interplay between periodic pinning with confinement effects, and how it affects the stabilization of different vortex arrangements and the changes in the phase diagram will surely produce new interesting results. These studies can be done in a variety of geometries both for the confinement and the pinning sites, thus allowing studies of the relative competition between these types of effects.

Interestingly, these experiments have relevance in fields as far removed as plasma physics, where ordered vortices appear in for instance cylindrical symmetric charged plasmas [205–207]. These charged plasmas are considered to be classical and therefore quantum effects are not expected to play a major role. A comparison of results in superconductors with those found in these charged plasmas may allow investigating quantum effects on vortex physics.

6.5. Ordered magnetic pinning arrays and HTSC

Up to this point, most work has focused towards understanding the effect that the pinning arrays have on the vortex physics and towards engineering novel situations and geometries of the pinning array which produce perhaps *a-priori* unexpected results. The particular superconductor under study played a minor effect. Its main role is to control the important relevant superconducting characteristic length scales (ξ and λ) without much change in the underlying physics. HTSC on the other hand open up a whole new avenue of research. The main reason for this is that HTSC exhibit a variety of vortex phases not present in LTSC (including vortex liquid, Bose or Bragg glasses) [208,209] due to the interplay between anisotropy, thermal fluctuations, and different kinds of disorder [2].

While disordered pinning (point and extended defects) has been thoroughly investigated in HTSC [2], only a few groups have investigated vortex dynamics with ordered pinning (in particular ordered arrays of "antidots") in these materials [210–212]. In addition, magnetic pinning in $YBa_2Cu_3O_7$ films has been demonstrated using a magnetic recording tape to induce a periodic potential in the vortex lattice with a several micron period [18,121,213,214]. Fabrication of regular arrays of submicrometric magnetic pinning centers is more complicated for HTSC [47] because the growth conditions of these complex oxides are usually incompatible with most standard nanofabrication techniques, as opposed to LTSC metals. However, HTSC such as the $REBa_2Cu_3O_{7-\delta}$ family (RE = rare earth) have some unique properties, which are unavailable in LTSC, that make the study of vortex dynamics with ordered artificial centers potentially very interesting. First, coherence and penetration length differ by several orders of magnitude [2,215]. Second, these layered HTSC compounds exhibit an intrinsic anisotropy which can be tailored by changing the oxygen content [2,216]. This together with large thermal fluctuations give rise to a rich variety of vortex phases [2,208] (vortex liquid, solid, glass, etc). Third, the intrinsic (disordered) pinning in HTSC thin films can be manipulated with substitutions of the ions [217,218], changes in the growth conditions (substrate, growth temperature, etc.), or even by ion irradiation [219]. Fourth, it is possible to epitaxially grow homostructural analogs with high structural quality using insulating (like $PrBa_2Cu_3O_{7-\delta}$) [220,221] or magnetic oxides (like $La_{0.67}Ca_{0.33}MnO_3$) [222]. Fifth, illumination by (spatially localized or global) light irradiation allows modifying the superconducting properties substantially [223,224]. These characteristics make investigation of these materials in conjunction with nanostructured pinning arrays quite attractive.

An important goal is separating pinning induced by local superconductivity suppression from pinning induced by magnetostatic interactions between vortices and stray magnetic fields. The superconducting coherence length ξ is the relevant length scale for the former mechanism, while the penetration length λ is relevant for the latter. Since these characteristic lengths are very different in HTSC, these are ideal materials to address this issue. Moreover, experiments could be done in which the magnetic state of the dots could be modified to induce changes on vortex pinning [42]. Especially interesting is the case in which dots are in the so-called "magnetic vortex state" [84,225], in which magnetization lies in-plane curling around the center of the dot and points out-of-plane (up or down) at the "vortex core". The orientation of these cores can be manipulated with external DC or AC applied magnetic field [215], and so, if magnetostatic interactions are important, the pinning landscape for superconducting vortices could be tuned by an external parameter [85–87].

Moreover, the rich variety of vortex phases exhibited by HTSC thin films [2,208], provides an interesting play ground for studies related to vortex phases and order–disorder competition. Some work has been done in LTSC [64], but the effect of ordered pinning on the stabilization of these different phases has not been experimentally investigated [219] in HTCS.

Finally, HTSC provide the ideal materials to weight vortex interactions and correlations: high upper critical fields (short coherence lengths) and much longer penetration lengths allow exploring regimes that span from low density vortex lattices with negligible vortex–vortex interactions to very dense lattices (as compared with the array of pinning centers) with strong inter-vortex interactions.

7. Summary

It is clear that the field of superconducting vortex pinning using artificial pinning structures is a very rich and fruitful area of research. Although considerable research has been done in the last 10 or so years, much remains to be done. This provides the ideal model system for the interaction of soft elastic with rigid lattices. The reason for this is that most if not all the parameters that are relevant to the physics can be manipulated and controlled at will through combined growth, lithography and external driving forces.

Acknowledgments

Work at UCSD was supported by the US NSF and US DOE. Financial support by the Spanish Ministerio de Educacion y Ciencia under grants NAN2004-09087, FIS2005-07392 and Consolider CSD2007-00010 and Comunidad de Madrid programa CITECNOMIK 2006-CM-ESP-0337-0505 is acknowledged. Work at Argonne was supported by the US DOE under contract no. DE-AC02-06CH1357.

References

[1] A.M. Campbell, J.E. Evetts, Adv. Phys. 21 (1972) 199.
[2] G. Blatter, M.V. Feigel'man, V.B. Geshkenbein, A.I. Larkin, V.M. Vinokur, Rev. Mod. Phys. 66 (1994) 1125.
[3] P.W. Anderson, Phys. Rev. Lett. 9 (1962) 309.
[4] J. Friedel, P.G. De Gennes, J. Matricon, Appl. Phys. Lett. 2 (1963) 119.
[5] W.W. Webb, Phys. Rev. Lett. 11 (1963) 191.
[6] J.W. Ekin, J. Appl. Phys. 62 (1987) 4829.
[7] C. Meingast, D.C. Larbalestier, J. Appl. Phys. 66 (1989) 5971.
[8] L. Civale, A.D. Marwick, T.K. Worthington, M.A. Kirk, J.R. Thompson, L. Krusin-Elbaum, Y. Sun, J.R. Clem, F. Holtzberg, Phys. Rev. Lett. 67 (1991) 648.
[9] A.T. Fiory, A.F. Hebard, S. Somekh, Appl. Phys. Lett. 32 (1978) 73.
[10] B. Pannetier, J. Chaussy, R. Rammal, J.C. Villegier, Phys. Rev. Lett. 53 (1984) 1845.
[11] O. Geoffroy, D. Givord, Y. Otani, B. Pannetier, F. Ossart, J. Magn. Magn. Mater. 121 (1993) 223.
[12] Y. Otani, B. Pannetier, J.P. Nozières, D. Givord, J. Magn. Magn. Mater. 126 (1993) 622.
[13] M. Baert, V.V. Metlushko, R. Jonckheere, V.V. Moshchalkov, Y. Bruynseraede, Phys. Rev. Lett. 74 (1995) 3269.
[14] J.-Y. Lin, M. Gurvitch, S.K. Tolpygo, A. Bourdillon, S.Y. Hou, J.M. Phillips, Phys. Rev. B 54 (1996) R12717.
[15] K. Harada, O. Kamimura, H. Kasai, T. Matsuda, A. Tonomura, V.V. Moshchalkov, Science 274 (1996) 1167.
[16] A. Gilabert, I.K. Schuller, V.V. Moshchalkov, Y. Bruynseraede, Appl. Phys. Lett. 64 (1994) 2885.
[17] L. Van Look, E. Rosseel, M.J. Van Bael, K. Temst, V.V. Moshchalkov, Y. Bruynseraede, Phys. Rev. B 60 (1999) R6998.
[18] G. Jung, S.J. Lewandowski, B.Ya. Shapiro, Y. Yuzhelevski, Physica C 332 (2000) 51.
[19] A.Y. Aladyshkin, A.A. Fraerman, S.A. Gusev, A.Y. Klimov, Y.N. Nozdrin, G.L. Pakhomov, V.V. Rogov, S.N. Vdovichev, J. Magn. Magn. Mater. 258–259 (2003) 406.
[20] A. Fraerman, S.A. Gusev, Yu.N. Nozdrin, A.V. Samokhvalov, S.N. Vdovichev, L. Fritzsch, E. Il'ichev, R. Stolz, Phys. Rev. B 73 (2006) R100503.
[21] S.N. Vdovichev, B.A. Gribkov, S.A. Gusev, E. Il'ichev, A.Yu. Klimov, Yu.N. Nozdrin, G.L. Pakhomov, V.V. Rogov, R. Stolz, A.A. Fraerman, JETP Lett. 80 (2004) 651.
[22] E. Dantsker, S. Tanaka, J. Clarke, Appl. Phys. Lett. 70 (1997) 2037.
[23] R. Wördenweber, A.M. Castellanos, P. Selders, Physica C 332 (2000) 27.
[24] L.M. Wang, C.-H. Hsieh, C.-C. Chang, IEEE Trans. Appl. Sup. 15 (2005) 1040.
[25] J.I. Martín, M. Vélez, J. Nogués, I.K. Schuller, Phys. Rev. Lett. 79 (1997) 1929.
[26] M. Tinkham, Introduction to Superconductivity, McGraw-Hill, New York, NY, 1996.
[27] S.H. Autler, J. Low Temp. Phys. 9 (1972) 241.
[28] I.F. Lyuksyutov, V.L. Pokrovsky, Adv. Phys. 54 (2005) 67.
[29] I.F. Lyuksyutov, V.I. Pokrovsky, Phys. Rev. Lett. 81 (1998) 2344.
[30] D.J. Morgan, J.B. Ketterson, Phys. Rev. Lett. 80 (1998) 3614.
[31] Y. Jaccard, J.I. Martín, M.-C. Cyrille, M. Vélez, J.L. Vicent, I.K. Schuller, Phys. Rev. B 58 (1998) 8232.
[32] J.I. Martín, M. Vélez, A. Hoffmann, I.K. Schuller, J.L. Vicent, Phys. Rev. Lett. 83 (1999) 1022.
[33] J.E. Villegas, M.I. Montero, C.-P. Li, I.K. Schuller, Phys. Rev. Lett. 97 (2006) 027002.
[34] A.V. Silhanek, W. Gillijns, V.V. Moshchalkov, B.Y. Zhu, J. Moonens, L.H.A. Leunissen, Appl. Phys. Lett. 89 (2006) 152507.
[35] J.E. Villegas, S. Savel'ev, F. Nori, E.M. González, J.V. Anguita, R. García, J.L. Vicent, Science 302 (2003) 1188.
[36] J.E. Villegas, E.M. González, M.P. González, J.V. Anguita, J.L. Vicent, Phys. Rev. B 71 (2005) 024519.
[37] A.V. Silhanek, W. Gillijns, V.V. Moshchalkov, V. Metlushko, B. Ilic, Appl. Phys. Lett. 89 (2006) 182505.
[38] A.V. Silhanek, W. Gillijns, V.V. Moshchalkov, V. Metlushko, F. Gozzini, B. Ilic, W.C. Uhlig, J. Unguris, Appl. Phys. Lett. 90 (2007) 182501.
[39] J.I. Martín, J. Nogués, K. Liu, J.L. Vicent, I.K. Schuller, J. Magn. Magn. Mater. 256 (2003) 449.
[40] M.I. Montero, K. Liu, O.M. Stoll, A. Hoffmann, J.J. Åkerman, J.I. Martín, J.L. Vicent, S.M. Baker, T.P. Russell, C. Leighton, J. Nogués, I.K. Schuller, J. Phys. D: Appl. Phys. 35 (2002) 2398.
[41] J.I. Martín, Y. Jaccard, A. Hoffmann, J. Nogués, J.M. George, J.L. Vicent, I.K. Schuller, J. Appl. Phys. 84 (1998) 411.
[42] M.J. Van Bael, J. Bekaert, K. Temst, L. Van Look, V.V. Moshchalkov, Y. Bruynseraede, G.D. Howells, A.N. Grigorenko, S.J. Bending, G. Borghs, Phys. Rev. Lett. 86 (2001) 155.

[43] M. Lange, M.J. Van Bael, Y. Bruynseraede, V.V. Moshchalkov, Phys. Rev. Lett. 90 (2003) 197006.
[44] Y. Fasano, J.A. Herbsommer, F. De la Cruz, F. Pardo, P.L. Gammel, E. Bucher, D.J. Bishop, Phys. Rev. B 60 (1999) R15047.
[45] Y. Fasano, M. Menghini, F. De la Cruz, G. Nieva, Phys. Rev. B 62 (2000) 15183.
[46] Y. Fasano, M. Menghini, Supercond. Sci. Technol. 21 (2008) 023001.
[47] W.J. Yeh, B. Cheng, B.L. Justus, Physica C 388–389 (2003) 433.
[48] Y. Nozaki, Y. Otani, K. Runge, H. Miyajima, B. Pannetier, J.P. Nozières, G. Fillion, J. Appl. Phys. 79 (1996) 8571.
[49] A. Hoffmann, P. Prieto, I.K. Schuller, Phys. Rev. B 61 (2000) 6958.
[50] Y. Fasano, M. De Seta, M. Menghini, H. Pastoriza, F. De la Cruz, Solid State Commun. 128 (2003) 51.
[51] M.J. Van Bael, K. Temst, V.V. Moshchalkov, Y. Bruynseraede, Phys. Rev. B 59 (1999) 14674.
[52] M.J. Van Bael, L. Van Look, M. Lange, J. Bekaert, S.J. Bending, A.N. Grigorenko, K. Temst, V.V. Moshchalkov, Y. Bruynseraede, Physica C 369 (2002) 97.
[53] J.I. Martín, M. Vélez, A. Hoffmann, I.K. Schuller, J.L. Vicent, Phys. Rev. B 62 (2000) 9110.
[54] A. Terentiev, D.B. Watkins, L.E. De Long, D.J. Morgan, J.B. Ketterson, Physica C 324 (1999) 1.
[55] C. Reichhardt, C.J. Olson, F. Nori, Phys. Rev. Lett. 78 (1997) 2648.
[56] C. Reichhardt, C.J. Olson, F. Nori, Phys. Rev. B 58 (1998) 6534.
[57] A. Terentiev, D.B. Watkins, L.E. De Long, D.D. Cooley, D.J. Morgan, J.B. Ketterson, Phys. Rev. B 61 (2000) R9249.
[58] C. Reichhardt, C.J. Olson, F. Nori, Phys. Rev. B 57 (1998) 7937.
[59] W.V. Pogosov, A.L. Rakhmanov, V.V. Moshchalkov, Phys. Rev. B 67 (2003) 014532.
[60] D.M. Silevitch, D.H. Reich, C.L. Chien, S.B. Field, H. Shtrikman, J. Appl. Phys. 89 (2001) 7478.
[61] G. Carneiro, Phys. Rev. B 66 (2002) 054523.
[62] M. Vélez, D. Jaque, J.I. Martín, F. Guinea, J.L. Vicent, Phys. Rev. B 65 (2002) 094509.
[63] M.F. Laguna, P.S. Cornaglia, C.A. Balseiro, Phys. Rev. B 66 (2002) 024522.
[64] J.E. Villegas, E.M. Gonzalez, Z. Sefrioui, J. Santamaria, J.L. Vicent, Phys. Rev. B 72 (2005) 174512.
[65] O. Daldini, P. Martinoli, J.L. Olsen, G. Berner, Phys. Rev. Lett. 32 (1974) 218.
[66] A.F. Hebard, A.T. Fiory, S. Somekh, IEEE Trans. Magn. 13 (1977) 589.
[67] A. Castellanos, R. Wördenweber, G. Ockenfuss, A.V.D. Hart, K. Keck, Appl. Phys. Lett. 71 (1997) 962.
[68] V. Metlushko, U. Welp, G.W. Crabtree, Z. Zhang, S.R.J. Brueck, B. Watkins, L.E. DeLong, B. Ilic, K. Chung, P.J. Hesketh, Phys. Rev. B 59 (1999) 603.
[69] U. Welp, Z.L. Xiao, V. Novosad, V.K. Vlasko-Vlasov, Phys. Rev. B 71 (2005) 014505.
[70] S. Raedts, A.V. Silhanek, M.J. Van Bael, V.V. Moshchalkov, Phys. Rev. B 70 (2004) 024509.
[71] L. Horng, J.C. Wu, P.C. Kang, P.H. Lin, T.C. Wu, Jpn. J. Appl. Phys. 42 (2003) 2679.
[72] G. Karapetrov, J. Fedor, M. Iavarone, D. Rosenmann, W.K. Kwok, Phys. Rev. Lett. 95 (2005) 167002.
[73] I.K. Marmorkos, A. Matulis, F.M. Peeters, Phys. Rev. B 53 (1996) 2677.
[74] A.I. Buzdin, Rev. Mod. Phys. 77 (2005) 935.
[75] M.V. Milosevic, S.V. Yampolskii, F.M. Peeters, Phys. Rev. B 66 (2002) 174519.
[76] M.W. Coffey, Phys. Rev. B 52 (1995) 9851.
[77] J.C. Wei, J.L. Chen, L. Horng, T.J. Yang, Phys. Rev. B 54 (1996) 15429.
[78] G. Carneiro, Phys. Rev. B 69 (2004) 214504.
[79] M.A. Kayali, Phys. Rev. B 71 (2005) 024515.
[80] S. Erdin, A.F. Kayali, I.F. Lyuksyutov, V. Pokrovsky, Phys. Rev. B 66 (2002) 014414.
[81] M.A. Kayali, Phys. Rev. B 69 (2004) 012505.
[82] S. Erdin, Phys. Rev. B 72 (2005) 014522.
[83] L. Van Look, M.J. Van Bael, K. Temst, J.G. Rodrigo, M. Morelle, V.V. Moschalkov, Y. Bruynseraede, Physica C 332 (2000) 356.
[84] R.P. Cowburn, D.K. Koltsov, A.O. Adeyeye, M.E. Welland, D.M. Tricker, Phys. Rev. Lett. 83 (1999) 1042.
[85] J.E. Villegas, C.-P. Li, I.K. Schuller, Phys. Rev. Lett. 99 (2007) 227001.
[86] A. Hoffmann, L. Fumagalli, N. Jahedi, J.C. Sautner, J.E. Pearson, G. Mihajlović, V. Metlushko, Phys. Rev. B 77 (2008) R060506.
[87] J.E. Villegas, K.D. Smith, Lei Huang, Yimei Zhu, R. Morales, Ivan K. Schuller, Phys. Rev. B 77 (2008) 134510.
[88] M.J. Van Bael, M. Lange, S. Raedts, V.V. Moshchalkov, A.N. Grigorenko, S.J. Bending, Phys. Rev. B 68 (2003) 014509.
[89] G. Teniers, M. Lange, V.V. Moschalkov, Physica C 369 (2002) 268.
[90] Q.H. Chen, G. Teniers, B.B. Jin, V.V. Moschalkov, Phys. Rev. B 73 (2006) 014506.
[91] D.J. Priour Jr., H.A. Fertig, Phys. Rev. Lett. 93 (2004) 057003.
[92] M.V. Milosevic, F.M. Peeters, Phys. Rev. Lett. 93 (2004) 267006.
[93] V. Pokrovsky, H. Wei, Phys. Rev. B 69 (2004) 104530.
[94] H. Wei, Phys. Rev. B 71 (2005) 144521.
[95] M.V. Milosevic, F.M. Peeters, Phys. Rev. Lett. 94 (2005) 227001.
[96] S. Erdin, Physica C 391 (2003) 140.
[97] D.J. Priour, H.A. Fertig, Physica C 404 (2004) 293.
[98] M.V. Milosevic, F.M. Peeters, Physica C 404 (2004) 246.
[99] H. Wei, Physica C 434 (2006) 13.
[100] Z.R. Yang, M. Lange, A. Volodin, R. Szymczak, V.V. Moshchalkov, Nat. Mater. 3 (2004) 793.
[101] M.V. Milosevic, F.M. Peeters, Europhys. Lett. 70 (2005) 670.
[102] A.V. Silhanek, W. Gillijns, M.V. Milosevic, A. Volodin, V.V. Moshchalkov, F.M. Peeters, Phys. Rev. B 76 (2007) R100502.
[103] W. Gillijns, M.V. Milosevic, A.V. Silhanek, V.V. Moshchalkov, F.M. Peeters, Phys. Rev. B 76 (2007) 184516.
[104] M. Lange, M.J. Van Bael, A.V. Silhanek, V.V. Moschalkov, Phys. Rev. B 72 (2005) 052507.
[105] V.V. Moshchalkov, M. Baert, V.V. Metlushko, E. Rosseel, M.J. Van Bael, K. Temst, Y. Bruynseraede, R. Jonckheere, Phys. Rev. B 57 (1998) 3615.
[106] A.N. Grigorenko, G.D. Howells, S.J. Bending, J. Bekaert, M.J. Van Bael, L. Van Look, V.V. Moshchalkov, Y. Bruynseraede, G. Borghs, I.I. Kaya, R.A. Stradling, Phys. Rev. B 63 (2001) 052504.
[107] A.V. Silhanek, L. Van Look, R. Jonckheere, B.Y. Zhu, S. Raedts, V.V. Moshchalkov, Phys. Rev. B 72 (2005) 014507.
[108] G.S. Mkrtchyan, V.V. Schmidt, Sov. Phys. JETP 34 (1972) 195.
[109] V. Metlushko, U. Welp, G.W. Crabtree, R. Osgood, S.D. Bader, L.E. DeLong, Z. Zhang, S.R.J. Brueck, B. Ilic, K. Chung, P.J. Hesketh, Phys. Rev. B 60 (1999) R12585.
[110] C. Reichhardt, N. Grønbech-Jensen, Phys. Rev. Lett. 85 (2000) 2372.
[111] C. Reichhardt, G.T. Zimanyi, R.T. Scalettar, A. Hoffmann, I.K. Schuller, Phys. Rev. B 64 (2001) 052503.
[112] E. Rosseel, M. Van Bael, M. Baert, R. Jonckheere, V.V. Moshchalkov, Y. Bruynseraede, Phys. Rev. B 53 (1996) R2983.
[113] B. Pannetier, J. Chaussy, R. Rammal, J.C. Villegier, Phys. Rev. Lett. 53 (1984) 1845.
[114] R.D. Parks, W.A. Little, Phys. Rev. 133 (1964) A97.
[115] L.E. De Long, S. Kryukov, V.V. Metlushko, V.V. Moshchalkov, Y. Bruynseraede, Physica C 404 (2004) 123.
[116] G.R. Berdiyorov, M.V. Milosevic, F.M. Peeters, Phys. Rev. B 74 (2006) 174512.
[117] R.P. Cowburn, A.O. Adeyeye, J.A.C. Bland, Appl. Phys. Lett. 70 (1997) 2309.
[118] L. Torres, L. Lopez Diaz, J. Iñiguez, Appl. Phys. Lett. 73 (1998) 3766.
[119] P. Vavassori, G. Gubiotti, G. Zangari, C.T. Yu, H. Yin, H. Jiang, G.J. Mankey, J. Appl. Phys. 91 (2002) 7992.
[120] A. Pérez-Junquera, G. Rodríguez-Rodríguez, M. Vélez, J.I. Martín, H. Rubio, J.M. Alameda, J. Appl. Phys. 99 (2006) 033902.
[121] Y. Yuzhelevski, G. Jung, C. Camerlingo, M. Russo, M. Ghinovker, B.Ya. Shapiro, Phys. Rev. B 60 (1999) 9726.
[122] A. García-Santiago, F. Sánchez, M. Varela, J. Tejada, Appl. Phys. Lett. 77 (2000) 2900.
[123] M. Lange, M.J. Van Bael, V.V. Moshchalkov, Y. Bruynseraede, Appl. Phys. Lett. 81 (2002) 322.
[124] M. Lange, M.J. Van Bael, L. Van Look, K. Temst, J. Swerts, G. Güntherodt, V.V. Moshchalkov, Y. Bruynseraede, Europhys. Lett. 53 (2001) 646;
M. Lange, M.J. Van Bael, L. Van Look, K. Temst, J. Swerts, G. Güntherodt, V.V. Moshchalkov, Y. Bruynseraede, Europhys. Lett. 57 (2002) 149.
[125] M. Lange, M.J. Van Bael, V.V. Moshchalkov, Y. Bruynseraede, J. Magn. Magn. Mater. 240 (2002) 595.
[126] M.J. Van Bael, S. Raedts, K. Temst, J. Swerts, V.V. Moshchalkov, Y. Bruynseraede, J. Appl. Phys. 92 (2002) 4531.
[127] S. Raedts, M.J. Van Bael, K. Temst, M. Lange, L. Van Look, J. Swerts, V.V. Moshchalkov, Y. Bruynseraede, Physica C 369 (2002) 258.
[128] T. Giamarchi, P. Le Doussal, Phys. Rev. B 55 (1997) 6577.
[129] C. Reichhardt, G.T. Zimanyi, N. Grønbech-Jensen, Phys. Rev. B 64 (2001) 014501.
[130] T. Joseph, C. Dasgupta, Phys. Rev. B 67 (2003) 214514.
[131] O.M. Stoll, M.I. Montero, J. Guimpel, J.J. Akerman, I.K. Schuller, Phys. Rev. B 65 (2002) 104518.
[132] A. Hoffmann, Ph.D. Thesis, University of California, San Diego, 1999.
[133] M.I. Montero, J.J. Åkerman, A. Varilci, I.K. Schuller, Europhys. Lett. 63 (2003) 118.
[134] M.I. Montero, O.M. Stoll, I.K. Schuller, Eur. Phys. J. B40 (2004) 459.
[135] M. Vélez, D. Jaque, J.I. Martín, M.I. Montero, I.K. Schuller, J.L. Vicent, Phys. Rev. B 65 (2002) 104511.
[136] J.E. Villegas, E.M. González, M.I. Montero, I.K. Schuller, J.L. Vicent, Phys. Rev. B 68 (2003) 224504.
[137] C.E. Chialvo, J. Guimpel, S. Reparaz, H. Pastoriza, Physica C 422 (2005) 112.
[138] J.E. Villegas, E.M. Gonzalez, M.I. Montero, I.K. Schuller, J.L. Vicent, Phys. Rev. B 72 (2005) 064507.
[139] J.E. Villegas, Ph.D. Thesis, Universidad Complutense de Madrid, 2005.
[140] S. Kolesnik, V. Vlasko-Vlasov, U. Welp, G.W. Crabtree, T. Piotrowski, J. Wróbel, A. Klimov, P. Przyslupski, T. Skoskiewicz, B. Dabrowski, Physica C 341–348 (2000) 1093.
[141] M.S. Welling, R.J. Wijngaarden, C.M. Aegerter, R. Wördenweber, P. Lahl, Physica C 404 (2004) 410.
[142] T. Giamarchi, P. Le Doussal, Phys. Rev. Lett. 76 (1996) 3408.
[143] C. Reichhardt, G.T. Zimanyi, Phys. Rev. B 61 (2000) 14354.
[144] V.I. Marconi, D. Domínguez, Phys. Rev. B 63 (2001) 174509.
[145] C.C. De Souza Silva, G. Carneiro, Phys. Rev. B 66 (2002) 054514.
[146] C. Reichhardt, F. Nori, Phys. Rev. Lett. 82 (1999) 414.
[147] A.V. Silhanek, L. Van Look, S. Raedts, R. Jonckheere, V.V. Moshchalkov, Phys. Rev. B 68 (2003) 214504.
[148] D. Jaque, E.M. González, J.I. Martin, J.V. Anguita, J.L. Vicent, Appl. Phys. Lett. 81 (2002) 2851.
[149] M.A. Kayali, V.L. Pokrovsky, Phys. Rev. B 69 (2004) 132501.
[150] M. Vélez, J.I. Martín, J.L. Vicent, Appl. Phys. Lett. 67 (1995) 3186.
[151] P. Reimann, Phys. Rep. 361 (2002) 57.
[152] R.D. Astumian, Science 276 (1997) 917.

[153] R.D. Astumian, P. Hänggi, Phys. Today 55 (2002) 33.
[154] I. Zapata, R. Bartussek, F. Sols, P. Hänggi, Phys. Rev. Lett. 77 (1996) 2292.
[155] C.-S. Lee, B. Jankó, L. Derényi, A.-L. Barabási, Nature 400 (1999) 337.
[156] J.F. Wambaugh, C. Reichhardt, C.J. Olson, F. Marchesoni, F. Nori, Phys. Rev. Lett. 83 (1999) 5106.
[157] B.Y. Zhu, F. Marchesoni, V.V. Moshchalkov, F. Nori, Phys. Rev. B 68 (2003) 014514.
[158] B.Y. Zhu, L. Van Look, V.V. Moshchalkov, F. Marchesoni, F. Nori, Physica E 18 (2003) 322.
[159] B.Y. Zhu, F. Marchesoni, F. Nori, Physica E 18 (2003) 318.
[160] S. Savel'ev, F. Nori, Nat. Mater. 1 (2002) 179.
[161] R. Wördenweber, P. Dymashevski, V.R. Misko, Phys. Rev. B 69 (2004) 184504.
[162] J. Van de Vondel, C.C. De Souza Silva, B.Y. Zhu, M. Morelle, V.V. Moshchalkov, Phys. Rev. Lett. 94 (2005) 057003.
[163] E.M. Gonzalez, M.P. Gonzalez, N.O. Núñez, J.E. Villegas, J.V. Anguita, M. Jaffa, A. Asenjo, J.L. Vicent, Physica C 437–438 (2006) 77.
[164] D.E. Shalom, H. Pastoriza, Phys. Rev. Lett. 94 (2005) 177001.
[165] D.Y. Vodolazov, F.M. Peeters, I.V. Grigorieva, A.K. Geim, Phys. Rev. B 72 (2005) 024537.
[166] Y. Togawa, K. Harada, T. Akashi, H. Kasai, T. Matsuda, F. Nori, A. Maeda, A. Tonomura, Phys. Rev. Lett. 95 (2005) 087002.
[167] D.Y. Vodolazov, B.A. Gribkov, S.A. Gusev, A.Yu. Klimov, Yu.N. Nozdrin, V.V. Rogov, S.N. Vdovichev, Phys. Rev. B 72 (2005) 064509.
[168] T.C. Wu, L. Horng, J.C. Wu, C.W. Hsiao, J. Kolacek, T.J. Yang, Physica C 437–438 (2006) 353.
[169] M. Morelle, N. Schildermans, V.V. Moshchalkov, Appl. Phys. Lett. 89 (2006) 112512.
[170] G. Carneiro, Physica C 432 (2005) 206.
[171] C.C. De Souza Silva, A.V. Silhanek, J. Van de Vondel, W. Gillijns, V. Metlushko, B. Ilic, V.V. Moshchalkov, Phys. Rev. Lett. 98 (2007) 117005.
[172] C.C. De Souza Silva, J. Van de Vondel, M. Morelle, V.V. Moshchalkov, Nature 440 (2006) 651.
[173] L. Dinis, E.M. González, J.V. Anguita, J.M.R. Parrondo, J.L. Vicent, New J. Phys. 9 (2007) 366.
[174] W. Gillinjs, A.V. Sihanek, V.V. Moschalkov, C.J. Olson Reichhardt, C. Reichhardt, Phys. Rev. Lett. 99 (2007) 247002.
[175] L. Dinis, E.M. González, J.V. Anguita, J.M.R. Parrondo, J.L. Vicent, Phys. Rev. B 76 (2007) 212507.
[176] S. Savel'ev, F. Marchesoni, F. Nori, Phys. Rev. Lett. 91 (2003) 010601.
[177] C.J. Olson Reichhardt, C. Reichhardt, Physica C 432 (2005) 125.
[178] E.M. Gonzalez, N.O. Nunez, J.V. Anguita, J.L. Vicent, Appl. Phys. Lett. 91 (2007) 062505.
[179] D. Cole, S. Bending, S. Savel'ev, A. Grigorenko, T. Tamegai, F. Nori, Nat. Mater. 5 (2006) 305.
[180] A. Behrooz, M.J. Burns, H. Deckman, D. Levine, B. Whitehead, P.M. Chaikin, Phys. Rev. Lett. 57 (1986) 368.
[181] J.M. Gordon, A.M. Goldman, J. Maps, D. Costello, R. Tiberio, B. Whitehead, Phys. Rev. Lett. 56 (1986) 2280.
[182] V. Misko, S. Savel'ev, F. Nori, Phys. Rev. Lett. 95 (2005) 177007.
[183] M. Kemmler, C. Gürlich, A. Sterck, H. Pöhler, M. Neuhaus, M. Siegel, R. Kleiner, D. Koelle, Phys. Rev. Lett. 97 (2006) 147003.
[184] V. Misko, S. Savel'ev, F. Nori, Phys. Rev. B 74 (2006) 024522.
[185] J. Eisenmenger, M. Oettinger, C. Pfahler, A. Plettl, P. Walther, P. Ziemann, Phys. Rev. B 75 (2007) 144514.
[186] R. Ramirez, A. Rahman, I.K. Schuller, Phys. Rev. B 30 (1984) 6208.
[187] P.T. Korda, M.B. Taylor, D.G. Grier, Phys. Rev. Lett. 89 (2002) 128301.
[188] S. Savel'ev, F. Marchesoni, F. Nori, Phys. Rev. E 70 (2004) 061107.
[189] D.Y. Vodolazov, F.M. Peeters, Phys. Rev. B 72 (2005) 172508.
[190] V.I. Marconi, Phys. Rev. Lett. 98 (2007) 047006.
[191] S. Savel'ev, F. Marchesoni, F. Nori, Phys. Rev. Lett. 92 (2004) 160602.
[192] C.P. Bean, J.D. Livingston, Phys. Rev. Lett. 12 (1964) 14.
[193] A.J. Moreno, S.O. Valenzuela, G. Pasquini, V. Bekeris, Phys. Rev. B 71 (2005) 132513.
[194] V.R. Misko, B. Xu, F.M. Peeters, Phys. Rev. B 76 (2007) 024516.
[195] A.K. Geim, I.V. Grigorieva, S.V. Dubonos, J.G.S. Lok, J.C. Maan, A.E. Filippov, F.M. Peeters, Nature 390 (1997) 259.
[196] V.A. Schweigert, F.M. Peeters, Phys. Rev. Lett. 83 (1999) 2409.
[197] I.V. Grigorieva, W. Escoffier, J. Richardson, L.Y. Vinnikov, S. Dubonos, V. Oboznov, Phys. Rev. Lett. 96 (2006) 077005.
[198] A. Kanda, B.J. Baelus, F.M. Peeters, K. Kadowaki, Y. Ootuka, Phys. Rev. Lett. 93 (2004) 257002.
[199] A.K. Geim, S.V. Dubonos, J.J. Palacios, I.V. Grigorieva, M. Henini, J.J. Schermer, Phys. Rev. Lett. 85 (2000) 1528.
[200] L.F. Chibotaru, A. Ceulemans, V. Bruyndoncx, V.V. Moshchalkov, Nature 408 (2000) 833.
[201] M.V. Milosevic, G.R. Berdiyorov, F.M. Peeters, Phys. Rev. Lett. 95 (2005) 147004.
[202] C. Carballeira, V.V. Moshchalkov, L.F. Chibotaru, A. Ceulemans, Phys. Rev. Lett. 95 (2005) 237003.
[203] M.V. Milosevic, G.R. Berdiyorov, F.M. Peeters, Phys. Rev. B 75 (2007) 052502.
[204] J.S. Neal, M.V. Milosevic, S.J. Bending, A. Potenza, L. San Emeterio, C.H. Marrows, Phys. Rev. Lett. 99 (2007) 127001.
[205] K.S. Fine, A.C. Cass, W.G. Flynn, C.F. Driscoll, Phys. Rev. Lett. 75 (1995) 3277.
[206] D.Z. Jin, D.H.E. Dubin, Phys. Rev. Lett. 80 (1998) 4434.
[207] D.Z. Jin, D.H.E. Dubin, Phys. Rev. Lett. 84 (2000) 1443.
[208] F. Bouquet, C. Marcenat, E. Steep, R. Calemczuk, W.K. Kwok, U. Welp, G.W. Crabtree, R.A. Fisher, N.E. Phillips, A. Schilling, Nature 411 (2001) 448.
[209] P. Gammel, Nature 411 (2001) 434.
[210] M. Pannetier, R.J. Wijngaarden, I. Fløan, J. Rector, B. Dam, R. Griessen, P. Lahl, R. Wördenweber, Phys. Rev. B 67 (2003) 212501.
[211] R. Wördenweber, P. Dymashevski, V.R. Misko, Phys. Rev. B 69 (2004) 184504.
[212] S. Ooi, T. Mochiku, S. Yu, E.S. Sadki, K. Hirata, Physica C 426–431 (2005) 113.
[213] Y. Yuzhelevski, G. Jung, Physica C 314 (1999) 163.
[214] M. Pannetier, R.J. Wijngaarden, R. Surdeanu, J.M. Huijbregste, K. Heeck, B. Dam, R. Griessen, Physica C 341–348 (2000) 1019.
[215] B. Van Waeyenberge, A. Puzic, H. Stoll, K.W. Chou, T. Tyliszczak, R. Hertel, M. Fähnle, H. Brückl, K. Rott, G. Reiss, I. Neudecker, D. Weiss, C.H. Back, G. Schütz, Nature 444 (2006) 461.
[216] Z. Sefrioui, D. Arias, M. Varela, J.E. Villegas, M.A. López de la Torre, C. León, G.D. Loos, J. Santamaría, Phys. Rev. B 60 (1999) 15423.
[217] J.L. McManus-Driscoll, S.R. Foltyn, B. Maiorov, Q.X. Jia, H. Wang, A. Serquis, L. Civale, Y. Lin, M.E. Hawley, M.P. Maley, D.E. Peterson, Appl. Phys. Lett. 86 (2005) 032505.
[218] R. Bernard, J.H. Pommereau, C. Gadois, S. Berger, D.G. Crété, J. Briatico, J.-P. Contour, O. Durand, J.-L. Maurice, J. Magn. Magn. Mater. 272 (2004) 150.
[219] C.J. Van der Beek, M. Konczykowski, L. Fruchter, R. Brusetti, T. Klein, J. Marcus, C. Marcenat, Phys. Rev. B 72 (2005) 214504.
[220] J.-M. Triscone, Ø. Fischer, Rep. Prog. Phys. 60 (1997) 1673.
[221] J.E. Villegas, Z. Sefrioui, M. Varela, E.M. Gonzalez, J. Santamaria, J.L. Vicent, Phys. Rev. B 69 (2004) 134505.
[222] Z. Sefrioui, D. Arias, V. Peña, J.E. Villegas, M. Varela, P. Prieto, C. León, J.L. Martinez, J. Santamaria, Phys. Rev. B 67 (2003) 214511.
[223] A. Gilabert, A. Hoffmann, M.G. Medici, I.K. Schuller, J. Supercond. 4 (2000) 1.
[224] V. Peña, T. Gredig, J. Santamaría, I.K. Schuller, Phys. Rev. Lett. 97 (2006) 177005.
[225] T. Shinjo, T. Okuno, R. Hassdorf, K. Shigeto, T. Ono, Science 289 (2000) 930.